Title
Regulated activation of the CUL3 ubiquitin ligase by a calcium-dependent co-adaptor complex

Author
McGourty, Colleen Amanda

Publication Date
2016

Peer reviewed|Thesis/dissertation

Regulated activation of the CUL3 ubiquitin ligase by a calcium-dependent co-adaptor complex

By Colleen Amanda McGourty

A dissertation submitted in partial satisfaction of the requirements for the degree of
Doctor of Philosophy
in
Molecular and Cell Biology
in the
GRADUATE DIVISION
of the
UNIVERSITY OF CALIFORNIA, BERKELEY

Committee in charge:
Professor Michael Rape, Chair
Professor Randy Schekman
Professor James Hurley
Professor James Olzmann

Spring 2016

Abstract

Regulated activation of the CUL3 ubiquitin ligase by a calcium-dependent co-adaptor complex

by

Colleen Amanda McGourty

Doctor of Philosophy in Molecular and Cell Biology

University of California, Berkeley

Professor Michael Rape, Chair

The small protein ubiquitin is an essential post-translational modification that regulates a vast number of cellular processes in eukaryotes. Through a cascade of enzymatic steps, ubiquitin is transferred from a ubiquitin activating enzyme (E1) to a ubiquitin conjugating enzyme (E2), which interacts with a ubiquitin ligase (E3) that stimulates transfer of ubiquitin to a substrate. Conjugation of ubiquitin to a substrate can result in a variety of outcomes, including changes in protein stability, localization, or binding partners. This modification is utilized to control a diversity of processes, including protein trafficking, cell division, DNA damage response, immune signaling, transcriptional regulation, and many others.

Cullin-RING-ligases (CRLs) are the largest class of ubiquitin E3 ligases. CRLs are comprised of one of seven Cullin scaffold proteins (CUL1, CUL2, CUL3, CUL4A, CUL4B, CUL5, and CUL7). The functions of these ligases are nearly as diverse as the function of ubiquitin itself. In particular, CUL3 has functions in developmental processes, mitosis, autophagy, organelle formation, endocytosis, and more. CUL3 exerts its many roles by pairing with at least 90 substrate receptors that recruit proteins to be ubiquitylated. When in complex with the substrate receptor KLHL12, CUL3 transfers a single ubiquitin to its substrate, SEC31, a structural component of the COPII vesicle coat that helps transport proteins from the endoplasmic reticulum to the Golgi apparatus. SEC31 ubiquitylation triggers an increase in COPII vesicle size, allowing for the packaging and transport of large proteins such as collagen.

In this work, I examine the mechanisms by which SEC31 ubiquitylation by $CUL3^{KLHL12}$ is regulated. $CUL3^{KLHL12}$ activity requires the calcium-binding proteins PEF1 and ALG2. PEF1 and ALG2 form a target-specific co-adaptor that acts as a calcium sensor. Together PEF1 and ALG2 are an integral part of the $CUL3^{KLHL12}$ ubiquitin ligase and allow for SEC31 targeting only in the presence of elevated cellular calcium concentrations. This translates a short-lived rise in cytosolic calcium levels into sustained ubiquitylation of SEC31, which in turn triggers formation of large COPII coats and collagen secretion. As calcium signaling is also known to control chondrocyte differentiation and collagen synthesis, the regulated activation of $CUL3^{KLHL12}$ could allow organisms to integrate collagen secretion into programs of craniofacial bone formation. This work shows that target-specific co-adaptors provide a mechanism for rapid and signal-dependent activation of CUL3 complexes important for human development and disease.

Table of Contents

Acknowledgements

Thank you to my family, friends, labmates, and professors whose support, encouragement, humor, and insight made this dissertation possible.

I owe many thanks to the MCB faculty at UC Berkeley. To my advisor, Professor Michael Rape - your enthusiasm and imagination helped me to push my experiments farther than I though possible. To the members of my thesis committee, Professors Randy Schekman, James Hurley, and James Olzmann – Thank you for your their valuable insight over the last several years. To Professor Diana Bautista – thank you for your expertise and experimental contributions to my dissertation, and Professor Jeremy Thorner – thank you for your continued encouragement and input.

To my labmates – it has been a privilege to work with you all. I joined the lab in part because I was touched by your camaraderie and support of each other, and I was not disappointed. In the early days - Achim, Aileen, Kate, Hermann, and Adam – you taught me everything I needed to know in lab. And later - the "legion of boom", Melissa, Elijah, Eugene – you were the source of unbelievable scientific discourse, but also a wealth of humor and understanding.

To Kate – you are a beautiful person. I'm honored that you've chosen to spend the last 4 years with me and that you're willing to stick around for whatever comes next. And to Megan – who would have thought that a conversation about "I love New York" would turn into such a profound friendship? You are two of the most incredible women I know. If I believed in fate or cosmic intervention, I would think the reason I landed in Berkeley instead of somewhere else was so that I would meet you both.

And finally, to my family – thank you for raising me to believe that I could achieve whatever I wanted and to value my education. At this point you're probably regretting it, having raised two ambitious children who both moved away to California for their careers, but Tess and I are appreciative nonetheless. Mom, Dad, Tess, Grandma – I love you all so much. Also Monty and Floyd, but I doubt they are reading this.

Chapter 1

Introduction

The Ubiquitin System

Ubiquitylation is an essential post-translational modification in eukaryotes that regulates a diversity of cellular processes including cell cycle progression, membrane trafficking, translation, cell fate determination and differentiation, response to DNA damage, inflammation, and others. Covalent attachment of ubiquitin to lysine residues of target proteins, or less commonly methionine or cysteine residues, has a variety of effects, depending on the nature of the ubiquitin modification. Monoubiquitylation, the attachment of a single ubiquitin to a protein substrate, can modulate intramolecular interactions by relieving autoinhibition or intermolecular interactions by altering protein-protein interactions. Additionally, monoubiquitylation can change intracellular protein localization and trafficking (Hicke, 2001). Individual ubiquitin moieties can also be linked to form chains, a process known as polyubiquitylation, in which a ubiquitin is covalently attached to one of seven lysines or the N-terminal methionine of another ubiquitin. The specific lysine or methionine linkages used to form these chains can dictate their function: proteins carrying ubiquitin chains linked through K48 or K11 of ubiquitin are targeted to the proteasome for degradation. K63 or N-terminal methionine-linked ubiquitin chains often recruit other binding partners and coordinate signaling events (Rahighi and Dikic, 2012).

The human genome encodes for around 600 ubiquitin ligases, and proteomic studies have detected ubiquitin modification of over 5000 unique proteins (Metzger et al., 2012). Determining the substrates of these 600 ubiquitin ligases, elucidating their mechanisms of action, and deciphering the functions of the vast varieties of ubiquitin modifications in the cell are active areas of research aimed at achieving a more thorough understanding of this "ubiquitous" post-translational modification.

Enzymatic Cascade

Conjugation of ubiquitin to target substrate proteins requires an enzymatic cascade consisting of three classes of proteins: two ubiquitin-activating enzymes (E1s), ~40 ubiquitin conjugating enzymes (E2s), and ~600 ubiquitin ligases (E3s). In the first step, ubiquitin is activated at its C-terminus and conjugated to the active site cysteine of the E1 enzyme in an ATP-dependent thioester formation reaction. This ubiquitin is then transferred to the active site cysteine of the E2 enzyme, after which the E2 enzyme pairs with an E3 ubiquitin ligase. There are two classes of E3 ubiquitin ligases: the "homologous to the E6-AP carboxy-terminus", or HECT-type E3 ligases, and the "really interesting new gene", or RING-type E3 ligases (Metzger et al., 2012). This work focuses on RING-type E3 ligases, which bind to both a substrate protein and a ubiquitin-charged E2 enzyme and stimulate the discharge of ubiquitin from the E2 to the target substrate (Dou et al., 2012; Plechanovova et al., 2012; Pruneda et al., 2012). As substrate binding to the E3 ligase is required to initiate ubiquitin transfer, E3 ligases are the major determinant in selecting which proteins are ubiquitylated. Binding of the substrate to the E3 ligase can be regulated by a variety of mechanisms including post-translational modifications such as target phosphorylation or hydroxylation (Petroski and Deshaies, 2005) and binding of small molecules to the E2 (Sheard et al., 2010; Tan et al., 2007). These mechanisms control when and where a particular substrate is ubiquitylated.

In this work, we report a mechanism in which binding of calcium ions to a subunit of an E3 ligase is required for substrate binding and ubiquitylation. This allows for tight spatial and temporal control of E3 ligase activity and ensures substrates are targeted only in the context of elevated cytosolic calcium concentrations.

Cullin-RING-ligases and CRL3

Cullin-RING-ligases (CRLs) are the largest class of ubiquitin E3 ligases. CRLs are comprised of one of seven Cullin scaffold proteins (CUL1, CUL2, CUL3, CUL4A, CUL4B, CUL5, and CUL7) (Petroski and Deshaies, 2005). The cellular processes regulated by these ubiquitin ligases are extremely diverse. CRLs facilitate ubiquitylation of substrates by binding both an E2 enzyme charged with ubiquitin and a substrate, thereby stimulating discharge of the ubiquitin from the E2 to the substrate (Dou, Buetow et al. 2012, Plechanovova, Jaffray et al. 2012, Pruneda, Littlefield et al. 2012). Cullin proteins bind neither substrate nor E2 enzyme directly, but instead do so through various adaptor proteins. Cullins bind E2 enzymes C-terminally through a RING domain-containing partner protein, either Rbx1 or Rbx2. Substrates are recruited through a large number of substrate receptor proteins that bind the N-terminus of the Cullin scaffold. For example, CRL1 recruits substrates through 69 distinct human F-box protein/Skp1 pairs, while CRL3 recruits substrates through ~100 BTB domain-containing proteins. (Lydeard et al., 2013)

When paired with an F-box protein, CRL1 facilitates primarily K48-linked polyubiquitylation of target substrates, resulting in their proteolytic degradation. In contrast, CRL3 has been shown to facilitate formation multiple ubiquitin topologies including mono-ubiquitylation K33-linked chains, and K48-linked chains (Jin et al., 2012; Liu et al., 2016; Yuan et al., 2014). In several instances, a single CRL3/BTB pair is thought to assemble different ubiquitin topologies on different substrates (Liu et al., 2016; Yuan et al., 2014). This diversity of activity residing within the same enzyme suggests factors such as additional binding proteins, small molecules, post-translational modifications, or unique properties of substrates themselves may contribute to the unique activities of CRL3 complexes. In this work, we identify two protein regulators of the ubiquitin ligase $CUL3^{KLHL12}$, the calcium-binding proteins PEF1 and ALG2, and show that calcium is required for full E3 ligase assembly and substrate modification.

CUL3 substrate binding through BTB proteins

Multiple classes of CRL3 substrate receptors bind substrates through a variety of mechanisms. This work focuses on the KLHL-type CRL3 substrate receptors, which share 3 domains: a BTB domain, a BACK domain, and 5 or 6 Kelch motifs. The BTB domain binds to CUL3 and undergoes homo- or hetero-dimerization with extremely high affinity (Genau et al., 2015; Sumara et al., 2007; Zhuang et al., 2009a). Similarly, the BACK domain is responsible for formation of higher-order oligomerization of substrate adaptors(Errington et al., 2012). The Kelch repeats form a beta-propeller structure that mediates substrate binding, often through loops that connect individual blades of the propeller (McMahon et al., 2006; Werner et al., 2015). Because of the geometry and oligomeric nature of CUL3 substrate receptors, multiple Kelch propellers are oriented in close apposition to each other, suggesting several mechanisms by which substrates could be targeted. First, a single substrate could contact multiple Kelch propellers, Second, a CUL3-substrate receptor complex could bind multiple substrates through its Kelch propellers at the same time (McMahon et al., 2006; Zhuang et al., 2009a).

The first of these models has been demonstrated for the CUL3 ubiquitin ligase $CUL3^{KEAP1}$, a regulator of the oxidative stress response, which ubiquitylates the transcription factor NRF2. KEAP1 is a KLHL-type CUL3 substrate receptor that dimerizes through its BTB domain. This positions the individual Kelch propellers near each other such that the KEAP1 dimer can bind two separate motifs of its substrate, NRF2. The "ETGE" motif of NRF2 contacts one Kelch propeller, and the "DLG" motif contacts the other. Engagement of both propellers by Nrf2 is required for its efficient polyubiquitylation and subsequent degradation (McMahon et al., 2006; Tong et al., 2006).

This suggests a general model whereby efficient targeting of substrates by CUL3 ubiquitin ligases requires substrate engagement at multiple sites. Based on our work, we hypothesize that the CUL3 ubiquitin ligase $CUL3^{KLHL12}$ recruits its substrate, SEC31A, through multiple binding sites. One KLHL12 Kelch propeller contacts SEC31 directly, and the neighboring Kelch propeller engages an adapter complex of two proteins, PEF1 and ALG2. Together these form an additional SEC31 binding site that is required for efficient ubiquitylation.

CUL3 function in development

CUL3 has been linked to multiple processes in organismal development. Accordingly, many CUL3 substrate receptors are transcriptionally up- and down- regulated upon differentiation of mouse and human embryonic stem cells (Jin et al., 2012). Perturbing the levels of several of these adaptors results in aberrant differentiation or cellular morphology of embryonic stem cells. The CUL3 substrate receptor KBTBD8 is downregulated upon human embryonic stem cell differentiation and is required for formation of the neural crest cell lineage in both human embryonic stem cells *in vitro* and in *Xenopus laevis* embryos (Werner et al., 2015). KLHL12 is similarly downregulated upon differentiation of mouse embryonic stem cells and is required for secretion of collagen. Inactivation of $CUL3^{KLHL12}$ function prevents trafficking of collagen and results in disrupted stem cell morphology due to improper contacts with the collagen-deficient extracellular matrix (Jin et al., 2012).

Aberrant activation of CUL3 is linked to human diseases such as autism, schizophrenia, myopathy, and hypertension through unknown mechanisms (Louis-Dit-Picard, Barc et al. 2012, Ravenscroft, Miyatake et al. 2013, De Rubeis, He et al. 2014). This indicates that CUL3 acts at multiple stages of development and implies that activation of CUL3 and specific adaptor proteins is under tight control. The mechanisms by which CUL3 activity is controlled in different developmental contexts are currently under investigation.

The studies presented here suggest a mechanism by which $CUL3^{KLHL12}$ may become activated in specific locations during development. Because $CUL3^{KLHL12}$ requires calcium ions, this ligase may become activated in areas of high calcium concentration, such as regions of developing bone. Accordingly, perturbation of this pathway in zebrafish causes a decrease in collagen-containing craniofacial structures.

Collagen trafficking through the secretory pathway

Previous work in the lab identified a role for $CUL3^{KLHL12}$ in the secretory pathway. Transmembrane proteins and proteins destined to be secreted from the cell are first inserted into the endoplasmic reticulum, then packaged into membrane-bound units called COPII vesicles, and finally trafficked to the Golgi apparatus. COPII vesicles are formed through the coordinated assembly of multiple proteins (Jensen and Schekman, 2011). First, the guanine nucleotide exchange factor SEC12 stimulates GTP uptake by the GTPase SAR1. GTP binding exposes an

amphipathic helix on SAR1, which inserts into the ER membrane. This serves to deform the ER membrane and to recruit the inner COPII coat complex comprised of SEC23 and SEC24. SEC23 is a GTPase activating protein (GAP) with weak activity toward Sar1, while SEC24 is a cargo binding protein that selects cargo to be packaged into the budding vesicle. Next, the outer COPII coat complex consisting of SEC31 and SEC13 is recruited. At the end of vesicle assembly, SEC31 binds to SEC23, stimulating its GAP activity, and causing SAR1 to hydrolyze GTP. This triggers disassembly of the COPII coat and completes the vesicle budding process.

The majority of COPII vesicles formed through this process are 60-80nm in diameter (Matsuoka et al., 1998). This size is sufficient to package most proteins that traffic through the secretory pathway with several notable exceptions including collagen, the lipid carrier molecules chylomicrons, and very low density lipoprotein (VLDL) particles (Jensen and Schekman, 2011). Collagen, a critical structural protein and major component of the extracellular matrix, assembles into a rigid trimeric triple-helix structure that can measure up to 400nm in length. Despite this discrepancy in size, collagen is transported from the ER to the Golgi through COPII vesicles, and mutations in genes encoding COPII proteins lead to collagen deposition defects, skeletal aberrations and developmental diseases, such as cranio-lenticulo-sutural dysplasia (Boyadjiev et al., 2006; Fromme et al., 2007). It was recently discovered that ubiquitylation can increase COPII vesicle size, allowing for efficient packing of collagen into COPII vesicles (Jin et al., 2012).

Ubiquitin-dependent regulation of collagen secretion

$CUL3^{KLHL12}$ was recently identified as a major determinant of cellular collagen secretion and COPII vesicle size. When activated, $CUL3^{KLHL12}$ catalyzes the mono-ubiquitylation of SEC31, a component of the outer COPII coat. This ubiquitylation drives the assembly of large COPII coats competent to package collagen. Perturbation of this function in mouse embryonic stem cells results in a cell compaction phenotype in which cells retain intracellular collagen and cannot properly attach to their substrate due to a lack of collagen in the extracellular matrix (Jin et al., 2012).

There are many open questions posed by this model. Namely, how is $CUL3^{KLHL12}$ activity specifically coordinated with the packaging of collagen into COPII vesicles? For the majority of COPII vesicles, cargo is recruited through four distinct isoforms of SEC24, which bind to transmembrane cargo and cargo receptors in the ER membrane (Miller et al., 2002; Miller et al., 2003). However, SEC24 is a soluble protein located in the cytosol and is not capable of contacting soluble collagen molecules in the ER lumen. This suggests the existence of a signal that communicates the presence of luminal collagen across the ER membrane to proteins in the cytosol. In at least one case, this signal is transmitted by a transmembrane protein: The ER transmembrane protein Tango1 and its partner protein cTAGE5 coordinate collagen packaging and COPII vesicle budding by binding type-VII collagen on the luminal side of the ER membrane and SEC23/24 on the cytoplasmic side (Saito et al., 2009; Saito et al., 2011). This pathway, however, is unique to type-VII collagen and does not explain the mechanisms by which other types of collagen are packaged. Our work suggests that the cytoplasmic signal that marks the presence of collagen in the ER lumen could be a small molecule like calcium that passes through the ER membrane, rather than a transmembrane protein signal.

Secondly, the mechanisms regulating the spatial and temporal activity of $CUL3^{KLHL12}$ were previously unknown. As described above, $CUL3^{KLHL12}$ activity must be specifically directed to sites of collagen export; it must ubiquitylate SEC31 on collagen-containing COPII

vesicles, but leave unmodified the SEC31 that is packaging other cargoes or is unassembled in the cytosol. This requirement for spatial regulation can be expanded to the organismal level. $CUL3^{KLHL12}$ is present in cell types that do not secrete collagen, and it ubiquitylates targets with diverse functions unrelated to COPII vesicle trafficking. $CUL3^{KLHL12}$ must remain inactive toward SEC31 in these cell types, but efficiently ubiquitylate it in collagen-secreting cells. The mechanisms by which this tissue-specific activation could occur are currently under investigation. Given the rapid timescale of COPII vesicle formation and ER-to- Golgi trafficking, it is likely that $CUL3^{KLHL12}$ is also under tight temporal control. The work here suggests that $CUL3^{KLHL12}$ is activated by ER calcium release, a rapid and transient cellular signaling event.

Chapter 2

Regulated activation of the CUL3 ubiquitin ligase by a calcium-dependent co-adaptor

Colleen A. McGourty, David Akopian, Carolyn Walsh, Amita Gorur, Achim Werner, Randy Schekman, Diana Bautista, and Michael Rape

Introduction

Metazoan development depends on carefully executed gene expression programs that instruct pluripotent stem cells to adopt specific fates at defined times and locations within the growing organism. A failure to establish the correct sequence of differentiation events, as caused by mutations in transcription factors, loss of epigenetic regulators, or exposure to environmental toxins, can result in severe birth defects (Lee and Young, 2013). This is illustrated by the neural crest, a collection of multipotent cells that emerge at the boundary of the neural plate and non-neural ectoderm and differentiate into various cell types, such as chondrocytes, melanocytes, or glia (Betancur et al., 2010; Green et al., 2015). Mutations in genes required for neural crest specification account for more than 500 human congenital diseases, and aberrant neural crest maintenance can lead to cancer, such as neuroblastoma or melanoma.

Early during development, neural crest cells migrate into the embryonic territory that is destined to become the craniofacial skeleton. These cranial neural crest cells differentiate into chondrocytes, which secrete an extracellular matrix that is largely composed of type II and type X collagen fibers (Cinque et al., 2015; Karsenty et al., 2009). During the final stages of endochondral bone formation, chondrocytes are replaced by osteoblasts that produce type I collagen (Alford et al., 2015). The collagen network secreted by chondrocytes and osteoblasts provides a blueprint for the deposition of calcium-phosphate crystals that endow the developing bone with the rigidity demanded of a major structural element of metazoan bodies (Karsenty et al., 2009). As expected from the important role of collagen during bone formation, problems with neural crest specification, chondrocyte differentiation, or collagen secretion have all been shown to result in aberrant craniofacial development (Twigg and Wilkie, 2015).

We recently identified the ubiquitin ligase CUL3 as a major determinant of neural crest specification and collagen secretion (Jin et al., 2012; Werner et al., 2015). CUL3 accomplishes these tasks by cooperating with distinct BTB domain containing substrate adaptors that recruit specific proteins for ubiquitylation (Furukawa et al., 2003; Geyer et al., 2003; Xu et al., 2003). When paired with its adaptor KBTBD8, CUL3 monoubiquitylates the nucleolar proteins TCOF1 and NOLC1, which establishes a ribosome biogenesis platform that includes RNA polymerase I (Werner et al., 2015). $CUL3^{KBTBD8}$-dependent changes in mRNA translation promote neural crest specification and chondrocyte differentiation (Werner et al., 2015), and mutations in TCOF1 or RNA polymerase I result in Treacher Collins Syndrome, a neurocristopathy characterized by aberrant craniofacial development (Dauwerse et al., 2011; Dixon and Dixon, 2004). Upon engaging the adaptor KLHL12, CUL3 catalyzes the monoubiquitylation of the COPII coat protein SEC31 (Jin et al., 2012). Ubiquitylation of SEC31 drives formation of large COPII carriers that are able to accelerate the traffic of collagen from the endoplasmic reticulum (Jin et al., 2012). Mutations in the SEC31-interactor SEC23A prevent collagen secretion during craniofacial chondrogenesis (Lang et al., 2006), which in humans results in cranio-lenticulo-sutural dysplasia (Boyadjiev et al., 2006; Fromme et al., 2007). Underscoring their function in a shared pathway, expression of KBTBD8 and KLHL12 is tightly co-regulated in human melanoma cells exposed to a small molecule disruptor of neural crest specification (White et al., 2011).

Aberrant regulation of CUL3 not only affects craniofacial development, but has also been associated with autism, schizophrenia, myopathy, and hypertension (De Rubeis et al., 2014; Louis-Dit-Picard et al., 2012; Ravenscroft et al., 2013). This indicates that CUL3 acts at multiple stages of human development and implies that activation of complexes between CUL3 and

specific adaptor proteins has to be under tight control. $CUL3^{KLHL12}$, the complex driving collagen secretion, illustrates the need for precise spatial regulation of CUL3 activation: as cells produce collagen in the ER and package it into vesicles that bud from the ER membrane (Gillon et al., 2012; Malhotra and Erlmann, 2015), $CUL3^{KLHL12}$ has to modify its substrate SEC31 at ER exit sites, but not in the cytoplasm. The localized activation of $CUL3^{KLHL12}$ on the cytosolic face of the ER membrane should ideally be coordinated with the sorting of collagen into budding vesicles, a reaction that occurs within the ER lumen. $CUL3^{KLHL12}$ also showcases the need for temporal regulation, as premature, delayed or reduced collagen secretion results in a spectrum of diseases, such as fibrosis, fragile bones and organismal aging (Ewald et al., 2015; Malhotra and Erlmann, 2015; Soret et al., 2015). It is likely that spatial and temporal control also ascertains proper activation of CUL3 complexes that operate in mitosis, autophagy, organelle formation, or endocytosis (Genau et al., 2015; Gschweitl et al., 2016; Lu and Pfeffer, 2013; Maerki et al., 2009; Pintard et al., 2003; Sumara et al., 2007; Yuan et al., 2014; Zhang et al., 2015). Previous studies had pointed to CUL3 neddylation, control of adaptor transcription, or autocatalytic adaptor degradation as systemic and often slow-acting mechanisms of CUL3 regulation (Duda et al., 2011; Jin et al., 2012; Schulman and Harper, 2009; Werner et al., 2015; Zhou et al., 2015). By contrast, how intracellular signals are translated into rapid activation of distinct CUL3-complexes is not known. As a consequence, mechanisms that allow cells to coordinate $CUL3^{KLHL12}$-activation with events that drive vesicle budding, collagen secretion, or bone formation remain to be discovered.

Here, we show that activation of $CUL3^{KLHL12}$ depends on a target-specific co-adaptor composed of two calcium-binding proteins, PEF1 and ALG2. The PEF1-ALG2 co-adaptor allows $CUL3^{KLHL12}$ to translate the short-lived release of calcium from the ER into the more persistent ubiquitylation of SEC31, which in turn drives COPII coat formation and collagen secretion. As calcium signaling also triggers chondrocyte differentiation and collagen synthesis (Lin et al., 2014; Tomita et al., 2002), the calcium-dependent activation of $CUL3^{KLHL12}$ could provide a mechanism to integrate collagen secretion into the developmental programs of bone formation. We propose that target-specific co-adaptors, such as PEF1-ALG2, endow metazoan organisms with the ability to precisely tune the activity of distinct CUL3 complexes in response to specific signaling events.

Results

PEF1 and ALG2 are novel components of the $CUL3^{KLHL12}$ ubiquitin ligase

To discover mechanisms of CUL3 activation, we focused on $CUL3^{KLHL12}$, which ubiquitylates the vesicle coat protein SEC31 and thereby promotes COPII coat formation and collagen secretion (Jin et al., 2012). We hypothesized that regulators of $CUL3^{KLHL12}$ might associate with KLHL12, SEC31, or both. To isolate such proteins, we utilized CompPASS mass spectrometry, an approach that was designed to identify interactions even if the binding partners are present at low abundance or associate with each other transiently (Huttlin et al., 2015; Sowa et al., 2009). We expressed KLHL12 or SEC31 in human embryonic kidney cells and compared their affinity-purification to approximately 150 immunoprecipitations that used the same epitope tag, cell line, and purification procedure (Figure 1A; Figure S1). Confirming earlier observations (Jin et al., 2012), these experiments showed that KLHL12 efficiently binds CUL3 and SEC31. In addition, we found that KLHL12 specifically associates with PEF1 and ALG2, two penta-EF-hand proteins that had been reported to interact with SEC31 (Yamasaki et al., 2006; Yoshibori et al., 2012); Lunapark, which stabilizes three-way junctions in the endoplasmic reticulum (Chen et al., 2015); the BTB-domain containing CUL3 adaptor KLHL26; RNF219, a ubiquitin ligase with links to Alzheimer's Disease (Rhinn et al., 2013); and the KELCH-domain directed HSP90 adaptor NUDCD3 (Taipale et al., 2014). Of these KLHL12-interactors, only PEF1 and ALG2, but not Lunapark, NUDCD3, or RNF219, were also identified in affinity-purifications of SEC31 (Figure 1A; Figure S1).

Proteomic dissection of PEF1 and ALG2 interaction networks confirmed the association of each protein with KLHL12 and CUL3 (Figure 1A; Figure S1). Accordingly, both HA-epitope tagged and endogenous PEF1 and ALG2 co-precipitated with $KLHL12^{FLAG}$, as determined by Western blot analysis (Figure 1B, C). Demonstrating that these interactions occurred at the endogenous level, the affinity-purification of SEC31 revealed its binding to PEF1, ALG2, and KLHL12 (Figure 1D). Notably, the reciprocal immunoprecipitation of endogenous ALG2 co-depleted KLHL12 from cell lysates, which suggests that most of KLHL12 exists in complexes with ALG2 (Figure 1E).

We had previously shown that KLHL12 binds its substrate SEC31 with sufficient stability to result in co-localization of $CUL3^{KLHL12}$ and SEC31 on large COPII coats (Jin et al., 2012). By performing sequential affinity-purification coupled to mass spectrometry we found that PEF1 and ALG2 also remained associated with KLHL12-SEC31 complexes (Figure 2A; Figure S1). Underscoring the stability of these interactions, Western blot analysis of sequential affinity-purifications revealed that endogenous PEF1 and ALG2 were enriched in KLHL12-SEC31 complexes (Figure 2B). Accordingly, PEF1 and ALG2, but not the alternative KLHL12-binding partner Lunapark, co-localized with KLHL12 and SEC31 on large COPII coats (Figure 2C, D; Figure S2A), which frequently marked compartments that also contained collagen (Figure 2E). Together, these results identify PEF1 and ALG2 as components of the $CUL3^{KLHL12}$ machinery and suggest that these proteins could be involved in COPII vesicle size control and collagen secretion.

PEF1 and ALG2 are required for $CUL3^{KLHL12}$-activity

To determine whether PEF1 and ALG2 are required for $CUL3^{KLHL12}$-activity, we depleted each protein by siRNAs and tested for the consequences of this treatment on substrate recognition by $CUL3^{KLHL12}$. As often observed with proteins that interact with each other (Jia et al., 2001), depletion of PEF1 also reduced ALG2 levels (Figure 3A). In addition, the loss of either PEF1 or ALG2 prevented the binding of endogenous KLHL12 or CUL3 to endogenous SEC31 (Figure 3A), which, as shown for ALG2, could be rescued by expressing an siRNA-resistant protein (Figure 6B). Similar observations were made if stably expressed KLHL12 was purified from cells that lacked either PEF1 or ALG2: both siRNA conditions abrogated the interaction between KLHL12 and SEC31, without affecting the binding of KLHL12 to the CUL3 core of the ubiquitin ligase (Figure S2B). Moreover, the interaction between endogenous SEC31 and KLHL12 was lost upon inactivation of the *PEF1* or *ALG2* genes using CRISPR/Cas9 (Figure 3B). We conclude that PEF1 and ALG2 are required for the stable binding of $CUL3^{KLHL12}$ to its key substrate, SEC31, in cells.

Given their importance for the association of $CUL3^{KLHL12}$ with SEC31, we asked whether PEF1 and ALG2 were also required for the ubiquitylation of SEC31. To address this question, we expressed His-tagged ubiquitin in a human cell line that allowed for inducible expression of KLHL12, purified ubiquitin conjugates under denaturing conditions, and tested for ubiquitylation of endogenous SEC31 by Western blotting. Consistent with previous findings using overexpressed SEC31 (Jin et al., 2012), the induction of KLHL12 resulted in the predominant monoubiquitylation of endogenous SEC31 (Figure 3C). $CUL3^{KLHL12}$ also catalyzed the formation of some higher molecular weight ubiquitin conjugates, which likely represented SEC31 molecules that were modified on multiple of its 65 lysine residues (Jin et al., 2012). In contrast, if these experiments were performed in the absence of PEF1 or ALG2, $CUL3^{KLHL12}$-dependent SEC31 ubiquitylation was not observed (Figure 3C).

As monoubiquitylation by $CUL3^{KLHL12}$ regulates COPII coat formation (Jin et al., 2012), we next depleted PEF1 or ALG2 from human embryonic kidney cells and asked whether this treatment affected the size of COPII coats. Similar to what we had observed before (Jin et al., 2012), the induction of KLHL12 in control cells resulted in large COPII structures that were marked by SEC31 and KLHL12 (Figure 3D, E; Figure S2C). By contrast, if cells were devoid of PEF1 or ALG2, KLHL12 did not co-localize with SEC31 and large COPII coats were not formed (Figure 3D, E; Figure S2B). The depletion of a separate KLHL12 binding partner, Lunapark, did not affect the size of COPII coats (Figure S2C), which underscores the specific requirement for PEF1 and ALG2 in these reactions.

Based on the function of large COPII vesicles in collagen transport (Jin et al., 2012; Malhotra and Erlmann, 2015), we finally asked whether loss of PEF1 and ALG2 affected the exit of newly synthesized collagen from the ER. To this end, we exposed human osteosarcoma cells to a heat pulse, which results in retention of pro-collagen-I in the ER, and then shifted these cells to lower temperatures to trigger a synchronous wave of collagen export from the ER (Venditti et al., 2012). Cells treated with control siRNAs rapidly transported collagen-I from the ER to the Golgi apparatus (Figure 3F). By contrast, the loss of PEF1 or ALG2 resulted in a profound delay of collagen-I arrival at the Golgi, with many cells displaying persistent collagen ER-staining throughout the time course of this experiment (Figure 3F). To investigate whether the delay in ER exit accordingly impaired collagen secretion from cells, we made use of HT1080 fibroblasts that constitutively express collagen-I, yet secrete it so efficiently that only minor collagen-I

levels are detected in cell lysates (Jin et al., 2012). As expected from our other experiments, the depletion of PEF1 or ALG2 from these HT1080 reporter cells led to a strong cellular retention of collagen (Figure 3G). Thus, PEF1 and ALG2 are required for $CUL3^{KLHL12}$ to stably engage SEC31, mediate SEC31 ubiquitylation, and trigger an increase in the size of COPII vesicles that drives collagen secretion. PEF1 and ALG2 are, therefore, essential for $CUL3^{KLHL12}$ activation in cells.

PEF1-ALG2 is a target-specific co-adaptor of $CUL3^{KLHL12}$

As a first step towards understanding the role of PEF1 and ALG2 in $CUL3^{KLHL12}$ activation, we determined how these proteins engage the $CUL3^{KLHL12}$ E3 ligase or its substrate SEC31. While analyzing the modification of SEC31, we noticed that $CUL3^{KLHL12}$ promoted the ubiquitylation of PEF1 (Figure 3C), which occurred on specific Lys residues in its EF-hand domain (Figure S3A). We did not observe ubiquitylation of PEF1 if cells expressed a KLHL12 variant that was unable to bind CUL3 or if endogenous KLHL12 had been depleted by siRNAs (Figure S3B, C). As purified PEF1 was also modified by recombinant $CUL3^{KLHL12}$ (Figure S3D), these experiments identified PEF1 as a substrate of $CUL3^{KLHL12}$ and suggested that PEF1 might bind $CUL3^{KLHL12}$ in a similar manner as SEC31. In accordance with this hypothesis, the same mutations in the Kelch repeat of KLHL12 that blocked SEC31 ubiquitylation ($KLHL12^{FG289AA}$) (Jin et al., 2012) also prevented $CUL3^{KLHL12}$ from binding to and ubiquitylating PEF1 (Figure 4A, B; Figure S3E, F). Moreover, increasing concentrations of PEF1 impaired SEC31 ubiquitylation by $CUL3^{KLHL12}$ *in vitro* (Figure S3G) and reduced the interaction between SEC31 and KLHL12 in cells (Figure S3H). These findings indicated that PEF1 and SEC31 access an overlapping surface on the Kelch repeat of KLHL12.

Truncation analyses revealed that PEF1 binds KLHL12 through amino-terminal Gly-Pro rich repeats (Figure S4A), whereas it uses its carboxy-terminal EF-hand domain to recognize ALG2 (Figure S4B). PEF1 therefore engages KLHL12 and ALG2 through different motifs, which enables it to bind both partners at the same time and thereby promote an interaction between $CUL3^{KLHL12}$ and ALG2 (Figure 4C). Conversely, ALG2 binds PEF1 through its fifth EF-hand (Figure S4C), while it uses its first EF-hand to associate with SEC31 (Figure S4D); in a similar manner to PEF1, ALG2 was able to mediate an interaction between PEF1 and SEC31 (Figure 4D). Finally, SEC31, which can bind KLHL12 and ALG2 directly (Jin et al., 2012; la Cour et al., 2013), also promoted an association between these two proteins (Figure 4E). Thus, KLHL12 binds PEF1, which in turn recognizes ALG2, which associates with SEC31. The latter could finally interact with another molecule of KLHL12 (Figure 4G).

As both KLHL12 and SEC31 are known to oligomerize (Errington et al., 2012; Fath et al., 2007; Zhuang et al., 2009b), the interactions described above likely occur in the same higher-order protein complex, as we had observed in cells (Figure 2B). PEF1-ALG2 and SEC31 could contact different subunits of a KLHL12 dimer; alternatively, KLHL12 bound to PEF1-ALG2 might associate with one SEC31 molecule, whereas a neighboring SEC31 subunit within the same coat could directly engage another KLHL12 dimer (Figure 4G). In each of these cases, we expected that the PEF1-ALG2 complex would stabilize, rather than compete for access to, $CUL3^{KLHL12}$-SEC31. In agreement with this notion, we found that CUL3 was recruited to ALG2-SEC31 complexes more efficiently in the presence of both PEF1 and ALG2 (Figure 4E), which resulted in slightly better ubiquitylation of SEC31 in a minimal reconstituted system (Figure 4F). In summary, these findings suggest that PEF1 and ALG2 endow $CUL3^{KLHL12}$ with an additional

binding site for SEC31, which enhances the ability of $CUL3^{KLHL12}$ to recognize and ubiquitylate this particular substrate. We conclude that PEF1-ALG2 acts as a target-specific co-adaptor of the $CUL3^{KLHL12}$ ubiquitin ligase.

PEF1-ALG2 mediate calcium-dependent activation of $CUL3^{KLHL12}$

The domain architecture of PEF1 and ALG2 immediately suggested a regulatory mechanism for $CUL3^{KLHL12}$ activation. PEF1 and ALG2 each contain five EF-hands, a domain that can undergo conformational changes in response to calcium-binding and thereby alter its protein interactions (Clapham, 2007). Indeed, previous work had indicated that calcium stabilizes the association of ALG2 with SEC31 (la Cour et al., 2013; Takahashi et al., 2015). As $CUL3^{KLHL12}$ requires the PEF1-ALG2 co-adaptor to bind and ubiquitylate SEC31 in cells, activation of $CUL3^{KLHL12}$ might therefore be calcium-dependent.

As a first test of this hypothesis, we used EGTA to chelate calcium in lysates of human embryonic kidney cells and determined the consequences of this treatment on binding partners of KLHL12 by mass spectrometry. Intriguingly, the chelation of calcium strongly reduced the association of KLHL12 with SEC13/31, PEF1, ALG2, CUL3, and Lunapark, whereas other KLHL12-binding partners were not affected (Figure 5A). When we analyzed affinity-purifications of stably expressed $KLHL12^{FLAG}$ or endogenous SEC31 by Western blotting, we found that the absence of calcium abolished SEC31-recognition by $CUL3^{KLHL12}$ (Figure 5B, C). Similar results were obtained in reconstitution experiments using recombinant proteins, which underscored the essential function of calcium during the formation of $CUL3^{KLHL12}$-PEF1-ALG2-SEC31 complexes (Figure 5D). The *in vitro* binding reactions further showed that $CUL3^{KLHL12}$-PEF1-ALG2-SEC31 complexes are dynamically regulated by physiologically relevant calcium concentrations: full $CUL3^{KLHL12}$-PEF1-ALG2-SEC31 complexes were efficiently formed at a calcium concentration of 130nM, while PEF1 was ejected at 800nM (Figure 5E). Thus, calcium levels within the range of those observed during ER calcium release (Clapham, 2007) are required for $CUL3^{KLHL12}$ to engage both PEF1-ALG2 and its key substrate SEC31.

We used our reconstituted system to determine the specific binding event within the $CUL3^{KLHL12}$-PEF1-ALG2-SEC31 complex that was regulated by calcium. While calcium was not required for the binding of PEF1 to KLHL12 or ALG2 (Figure 5D; Figure S4A), its removal specifically prevented the interaction between ALG2 and SEC31 (Figure S5A). The chelation of calcium in cell lysates accordingly abolished the binding of ALG2 to SEC31, whereas PEF1 and $CUL3^{KLHL12}$ remained associated (Figure 6A). In line with these and previous observations (la Cour et al., 2013; Takahashi et al., 2015), mutating residues in the first EF-hand of ALG2 that prevented calcium binding ($ALG2^{E47A}$) or destroyed a surface exposed by calcium ($ALG2^{F60A}$) also inhibited the interaction between ALG2 and SEC31 (Figure 5E; Figure S4D). By contrast, mutating the calcium-binding site in EF-hand 3 or deleting the PEF1-binding EF-hand 5 of ALG2 did not affect the association between ALG2 and SEC31.

These observations implied that ALG2 has to be loaded with calcium in order to allow $CUL3^{KLHL12}$ recruit SEC31. To test this hypothesis, we depleted ALG2 from human embryonic kidney cells and then expressed either siRNA-resistant wild-type ALG2 or variants of ALG2 that were deficient in calcium-binding ($ALG2^{E47A}$) or had a mutant hydrophobic surface exposed by calcium ($ALG2^{F60A}$). We also produced an ALG2 mutant that was defective in its association with PEF1 and thus, was unable to integrate into the $CUL3^{KLHL12}$ ligase ($ALG2^{\Delta EF5}$). Next, we affinity-purified endogenous SEC31 and monitored its interaction with $CUL3^{KLHL12}$. As we had

seen before, the depletion of ALG2 abrogated the association of SEC31 with $CUL3^{KLHL12}$, which was rescued by expression of siRNA-resistant wild-type ALG2 (Figure 6B). In contrast, $ALG2^{E47A}$, $ALG2^{F60A}$, or $ALG2^{\Delta EF5}$ did not reinstate recognition of SEC31 by $CUL3^{KLHL12}$ in ALG2-depleted cells (Figure 6B), and the expression of $ALG2^{E47A}$ in fact had a dominant negative effect on the formation of KLHL12-SEC31 complexes (Figure S5B). These findings show that calcium-binding to ALG2 as well as integration of ALG2 into the $CUL3^{KLHL12}$ complex are required for $CUL3^{KLHL12}$ activation towards SEC31 in cells.

To establish whether ALG2 is sufficient to mediate the effects of calcium on substrate recognition by $CUL3^{KLHL12}$, we engineered a SEC31-ALG2 fusion that mimics a constitutive, rather than calcium-dependent, interaction between both proteins. We expressed the SEC31-ALG2 fusion in cells and monitored its ability to engage $CUL3^{KLHL12}$ in the presence or absence of calcium. Importantly, we found that $CUL3^{KLHL12}$ was able to engage the SEC31-ALG2 fusion even in the absence of calcium (Figure 6C), which strongly suggests that the formation of the SEC31-ALG2 interface is the major event in $CUL3^{KLHL12}$ activation that is controlled by calcium. Interestingly, the SEC31-ALG2 fusion was poly-, rather than monoubiquitylated in cells (Figure 6D), which was dependent upon CUL3 (Figure S5C) and induced the proteasomal degradation of the fusion (Figure S5D). Together, these findings identify $CUL3^{KLHL12}$ as a calcium-dependent ubiquitin ligase and show that calcium binding to ALG2 is required and sufficient to establish recognition of the key $CUL3^{KLHL12}$-substrate SEC31 in cells. In addition to providing a potential mechanism of regulation, the calcium-dependent interactions of $CUL3^{KLHL12}$ ensure that SEC31 is decorated with the biologically active modification, monoubiquitylation.

Calcium release from the ER increases the size of COPII vesicles

The discovery of ALG2 as a calcium sensor for $CUL3^{KLHL12}$ allowed us to monitor the kinetics of CUL3 activation in real time. In these experiments, we monitored the localization of stably expressed GFP-tagged ALG2 (^{GFP}ALG2) in response to abrupt changes in intracellular calcium concentrations. ALG2 was the only subunit of $CUL3^{KLHL12}$ that could be labeled with a fluorescent protein without compromising function. Moreover, as shown by affinity-purification of endogenous proteins, the vast majority of KLHL12 was associated with ALG2 (Figure 1F), suggesting ^{GFP}ALG2-localization can serve as a proxy for $CUL3^{KLHL12}$ activation.

To rapidly change calcium concentrations, we exposed cells kept in 2mM calcium to ionomycin, which triggers calcium release from intracellular stores followed by sustained calcium influx from the environment. Under these conditions, the global calcium concentration started at 101 $^{+}$/- 15nM, reached 130 nM (i.e. the calcium concentration at which efficient ALG2-SEC31 binding was observed in vitro) within 5 $^{+}$/- 1.2 seconds, and peaked at 1.4 $^{+}$/- 0.32 µM in 67 $^{+}$/- 4 seconds. Alternatively, we solely triggered calcium release from intracellular stores by ionomycin (i.e. in the presence of calcium chelators in the medium) or histamine, a physiological compound that triggers IP3-dependent calcium release from the ER. The latter two approaches resemble the physiological situation of signal-dependent calcium release from the ER and produce a rise in cytosolic calcium levels that quickly dissipates through re-import of calcium into the ER or buffering by cytosolic calcium-binding proteins (Clapham, 2007). Under these conditions, we observed a resting intracellular calcium concentration of 61 $^{+}$/- 18 nM, which increased to 130 nM in 5.2 $^{+}$/- 1.9 seconds. The maximum calcium concentration of 458 $^{+}$/- 101 nM was observed after 32 $^{+}$/- 14 seconds.

In line with previous observations (la Cour et al., 2007), the abrupt increase in calcium concentrations caused the rapid re-localization of ^{GFP}ALG2 from a cytoplasmic pool to vesicular structures (Figure 7A, B; Movie S1-3) that co-localized with SEC31 (Figure S6A). Importantly, the time it took ^{GFP}ALG2 to relocate to COPII coats (~5 seconds) coincided well with the time required for cytosolic calcium concentrations to reach 130 nM. Whereas cells grown in calcium-containing medium and exposed to ionomycin showed a more persistent COPII recruitment of ^{GFP}ALG2, the physiological release of calcium from the ER produced a rapid, but also reversible targeting of ^{GFP}ALG2 to COPII coats (Figure 7A). The time of co-localization between ^{GFP}ALG2 and COPII coats mirrored the duration of elevated cytosolic calcium levels in cells, and it matched the time that was required by CUL3^{KLHL12} to ubiquitylate SEC31 and PEF1 (Figure S6B). Mutating the calcium-binding site (ALG2^{E47A}), the calcium-dependent hydrophobic surface (ALG2^{F60A}), or the PEF1-binding motif that connects ALG2 to CUL3^{KLHL12} (ALG2$^{\Delta EF5}$) disrupted the calcium-dependent recruitment of ALG2 to COPII vesicles (Figure 7B). Together, these findings indicate that a short-lived rise in cytosolic calcium rapidly targets CUL3^{KLHL12}-PEF1-ALG2 to its key substrate, SEC31, where it resides sufficiently long to produce the more persistent SEC31 monoubiquitylation.

In addition to providing evidence for the calcium-dependent activation of the CUL3^{KLHL12}, our observations raised the possibility that cells could use calcium signaling to adjust the size of their COPII coats to altered conditions; for example, cells could activate CUL3^{KLHL12}, and thus promote collagen secretion, in response to high calcium levels that are found in the ossification centers of developing bones. To test for calcium- and ubiquitin-dependent regulation of COPII coat size, we increased the calcium concentration in cells that expressed FLAG-epitope tagged KLHL12 and then used automated image analysis to determine whether the size of KLHL12-positive COPII structures changed in response to this treatment. Strikingly, we observed a significant increase in average COPII coat size and the number of large COPII vesicles within a minute of a rise in cytosolic calcium levels (Figure 7C-E). COPII coats continued to grow to almost twice their original size but then plateaued, which is indicative of a process that is limited by at least one intracellular component. Indeed, this regulatory circuit operated through CUL3-dependent ubiquitylation, as either depletion of either CUL3 or the CUL3^{KLHL12} co-adaptor PEF1-ALG2 barred calcium from invoking an increase in the size or number of large COPII vesicles (Figure 7E). The calcium-dependent activation of CUL3^{KLHL12}, therefore, triggers the formation of large COPII coats that are required to initiate the process of collagen secretion.

Discussion

The intricate sequence of differentiation events that establishes the human body plan requires that developmental signals are sent and received at precise times and locations within the growing organism. Studies on phosphorylation-dependent signal transduction cascades have revealed how kinases use scaffolds or adaptors to target specific substrates (Langeberg and Scott, 2015). Reminiscent of such kinases, the ubiquitin ligase CUL3, whose mutation has been associated with autism, schizophrenia, myopathies and hypertension, can pair with ~90 distinct substrate adaptors, yet how different CUL3 complexes are turned on at the right time or place is not known. Here, we show that activation of CUL3 and its adaptor KLHL12 requires a target-specific co-adaptor composed of the calcium-binding proteins PEF1 and ALG2. This co-adaptor allows $CUL3^{KLHL12}$ to translate a transient rise in cytosolic calcium levels into the more persistent ubiquitylation of the COPII protein SEC31, which in turn triggers an increase in COPII coat size and promotes collagen secretion. Our studies suggest that target-specific co-adaptors provide a means for the rapid and signal-dependent activation of specific CUL3 complexes that are critical for human development and disease.

Target-specific co-adaptors control substrate recognition by CUL3

Prior to their identification as subunits of a CUL3 ubiquitin ligase, PEF1 and ALG2 were known to form a stable complex (Jia et al., 2001), which based on quantitative proteomics performed in fibroblasts was present at equimolar levels with SEC31, and in excess over CUL3 or KLHL12 (Schwanhausser et al., 2011). Indeed, our affinity-purification experiments revealed that the majority of endogenous $CUL3^{KLHL12}$ is bound to ALG2. These findings indicate that PEF1 and ALG2 are able to regulate most, if not all, $CUL3^{KLHL12}$ assemblies in cells.

The PEF1-ALG2 complex is anchored on $CUL3^{KLHL12}$ by a proline-rich domain in PEF1, which occupies the same KLHL12 surface that is also recognized by SEC31. Consistent with this notion, the interaction of PEF1 with KLHL12 results in ubiquitylation of PEF1 by $CUL3^{KLHL12}$. Mutation of the lysine residues in PEF1 that are ubiquitylated by $CUL3^{KLHL12}$ did not have overt effects on COPII size (data not shown), which might indicate that ubiquitylation of PEF1 is a bystander modification or has a role in fine-tuning or limiting the activity of $CUL3^{KLHL12}$. Although PEF1 that is overexpressed in the absence of ALG2 may compete with SEC31 for access to KLHL12, *in vitro* reconstitution experiments and sequential affinity-purification from cells showed that the PEF1-ALG2 complex engages the same $CUL3^{KLHL12}$-assembly as SEC31. As KLHL12 and SEC31 are oligomeric proteins, distinct subunits of a KLHL12 dimer might interact with SEC31 and PEF1-ALG2-SEC31 at the same time (Figure 4G). It is also possible that KLHL12 and KLHL12-PEF1-ALG2 target neighboring SEC31 molecules within the same COPII coat. Independent of the mechanism, whose dissection will depend on structural analyses, the PEF1-ALG2 complex supports SEC31 recognition by $CUL3^{KLHL12}$ *in vitro*, and is essential for SEC31 binding, ubiquitylation, and COPII regulation in cells. We conclude that PEF1 and ALG2 function as SEC31-specific co-adaptor of $CUL3^{KLHL12}$.

Why does the cellular $CUL3^{KLHL12}$ depend on the PEF1-ALG2 co-adaptor for recognition of SEC31, even though $CUL3^{KLHL12}$ can directly bind and ubiquitylate SEC31 *in vitro* (Jin et al., 2012)? Whereas reconstituted systems only interrogate the interaction between $CUL3^{KLHL12}$ and few substrates, i.e. PEF1 and SEC31, cells contain many more proteins that can compete for recognition by $CUL3^{KLHL12}$ or SEC31. Such factors include other $CUL3^{KLHL12}$ substrates, such as Dishevelled, whose ubiquitylation by $CUL3^{KLHL12}$ induces its proteasomal degradation during

Wnt signaling (Angers et al., 2006), or Lunapark, an ER-resident protein that we identified as a KLHL12 partner in this study. Alternatively, interactors of SEC31, such as the COPII coat component SEC23 or its very abundant binding partner SEC23IP (Figure S1), might suppress SEC31 ubiquitylation until calcium is released from the ER to signal a need for larger COPII vesicles to transport collagen. It is also possible that phosphorylation of SEC31, which has been described in cells (Koreishi et al., 2013), but is absent from our reconstituted system, destabilizes the SEC31-KLHL12 interface to impose a requirement for PEF1 and ALG2. The PEF1-ALG2 co-adaptor is therefore particularly important under physiological conditions that allow for multiple components to compete for access to $CUL3^{KLHL12}$ or its cognate substrate SEC31.

Recent findings raise the possibility that also other CUL3 complexes might depend on target-specific co-adaptors for activation. Indeed, we showed that the CUL3 complex that guides neural crest specification, $CUL3^{KBTBD8}$, requires β-arrestin for activity (Werner et al., 2015). Akin to the phenotypes of PEF1- or ALG2-depletion, loss of β-arrestin abolished the recognition and monoubiquitylation of the $CUL3^{KBTBD8}$-substrates TCOF1- and NOLC1. β-arrestin typically associates with phosphorylated peptides, a function that is best understood in the context of its role as a desensitizer of GPCR-dependent signaling (Kovacs et al., 2009). It is tempting to speculate that β-arrestin is a target-specific co-adaptor of $CUL3^{KBTBD8}$ that establishes phosphorylation-dependent control over TCOF1- and NOLC1-ubiquitylation during neural crest specification. In addition to KLHL12 and KBTBD8, large-scale proteomic studies had pointed to additional CUL3 adaptors that stably associate with proteins enriched in interaction modules, and we believe that many of these proteins function as co-adaptors rather than substrates (Huttlin et al., 2015). We therefore anticipate that target-specific co-adaptors provide a general mechanism to control substrate recognition and ubiquitylation by specific variants of the CUL3 ubiquitin ligase.

Calcium-dependent coordination of collagen synthesis and secretion

By rendering the recognition of SEC31 reliant on PEF1-ALG2, $CUL3^{KLHL12}$ establishes calcium-dependent regulation of COPII coat size. As seen by quantitative measurements of calcium concentrations in our binding reactions, the key event in substrate binding by $CUL3^{KLHL12}$, i.e. formation of the ALG2-SEC31 interface, occurs very efficiently at 130nM calcium. Thus, the $CUL3^{KLHL12}$-PEF1-ALG2 axis is sufficiently sensitive to respond to the physiological changes in cytosolic calcium concentrations that are imposed by ER calcium release (Clapham, 2007), a finding that was corroborated by live cell imaging of ^{GFP}ALG2 expressed cells that were exposed to histamine (Figure 7A). Our video microscopy experiments also showed that ALG2 is recruited to SEC31 within seconds of calcium-release from the ER, revealing that this machinery functions on the time-scales imposed by intracellular calcium signaling. Interestingly, higher calcium concentrations of ~800nM and above, which can be observed in ER-proximal calcium microdomains (Petersen, 2015), resulted in the ejection of PEF1 from $CUL3^{KLHL12}$. It is possible that PEF1 initially allows ALG2-bound SEC31 to recognize KLHL12, thereby effectively increasing the local concentration of SEC31 on $CUL3^{KLHL12}$. If calcium levels keep rising, the subsequent loss of PEF1 from $CUL3^{KLHL12}$ might open up additional binding sites for SEC31 to directly bind its ubiquitin ligase, resulting in more efficient SEC31 ubiquitylation. $CUL3^{KLHL12}$ is, therefore, a ubiquitin ligase that is dynamically regulated by calcium signaling.

As illustrated by the unfolded protein response (Wang and Kaufman, 2014), cells often use calcium signaling to connect events that occur in the ER lumen with pathways that operate in the cytosol. In most cases, the calcium signal released from the ER dissipates on a time scale of

seconds (Clapham, 2007). While this might allow for enzyme activation, as seen with $CUL3^{KLHL12}$ or calcium-dependent kinases (Stratton et al., 2013), it is difficult to envision how such dynamic signaling directly results in large-scale cellular changes, such as those required to build a large vesicle coat. By activating an E3 ligase and thereby triggering the covalent modification of a coat component, cells could translate a short-lived ER-proximal calcium signal into a more persistent change to a cytosolic protein that is then read out by effector proteins that build large COPII coats. We, therefore, propose that $CUL3^{KLHL12}$ establishes a persistent domain of COPII growth triggered by rapid calcium signaling from the ER.

Our observation that a signal originating from the ER can activate a cytosolic E3 ligase has important implications for the mechanism of collagen secretion. Specifically, our work raises the possibility that cells could employ calcium signaling to coordinate the packaging of collagen into budding vesicles, which occurs in the ER lumen, with the cytosolic regulation of COPII coat size (Malhotra and Erlmann, 2015). In this scenario, calcium channels that reside in proximity to ER exit sites might be activated by cellular attempts to package collagen into a COPII vesicle. The ensuing localized release of calcium, a process previously implicated in the formation of calcium microdomains at the ER membrane (Petersen, 2015; Rizzuto and Pozzan, 2006), could turn on a defined population of $CUL3^{KLHL12}$, and thus, allow for the specific ubiquitylation of SEC31 molecules that are present at the correct location to participate in collagen trafficking. In support of this hypothesis, ALG2 does not only function as the calcium sensor of $CUL3^{KLHL12}$, but it has recently been shown to also promote binding of SEC31 to SEC23 (la Cour et al., 2013). SEC23 is a COPII coat component that associates with SEC24, which in turn binds to the collagen VII-specific receptor of COPII, TANGO (Saito et al., 2009). Thus, recruitment of collagen into budding vesicles and ubiquitin-dependent formation of large COPII coats could indeed be coupled processes. To establish whether calcium signaling provides the necessary coordination, it will be important to identify the nature, localization, and regulation of the calcium transporters that participate in COPII vesicle size control and collagen secretion.

We anticipate that organisms employ the calcium-dependent activation of $CUL3^{KLHL12}$ to coordinate collagen secretion with other steps in their development. As metazoans store most of their calcium in bones, $CUL3^{KLHL12}$-dependent collagen secretion should be active in chondrocytes that reside close to the calcium-rich ossification centers of developing bone structures. Indeed, these chondrocytes were previously found to be most active in secreting collagen during bone formation (Karsenty et al., 2009). Calcium also activates a transcription factor cascade that is centered on NF-AT and SOX9 and drives chondrocyte differentiation as well as transcription of collagen genes (Lin et al., 2014; Tomita et al., 2002). This role of calcium in bone formation is underscored by fetal alcohol spectrum disorders, in which aberrant calcium signaling results in problems with neural crest specification and craniofacial development (Smith et al., 2014). By using the same signal, calcium, to activate chondrocyte differentiation, collagen synthesis and $CUL3^{KLHL12}$-dependent collagen secretion, metazoan organisms could ensure that these processes are coordinated with each other to establish robust craniofacial development.

Methods

Plasmids

For transient expression in human cells and *in vitro* transcription/translation, the following constructs were cloned into pCS2+: KLHL12^{FLAG}, PEF1^{FLAG}, KLHL12^{HA}, PEF1^{HA}, ^{HA}Sec31, ^{HA}ALG2, Lunapark^{HA}, ^{6xHIS}Ubiquitin, dominant negative CUL3 (residues 1-450), PEF1 N-terminus (residues 1-109) PEF1 C-terminus (residues 109-284). Sec31A was cloned into RFP-pRK5 (a gift from Rosalie Lawrence and Roberto Zoncu, UC Berkeley). Sec31A-ALG2 fusion constructs were generated by simultaneously ligating ^{HA}Sec31A and ALG2 inserts with complementary restriction sites into pCS2+.

For stable expression, ^{HA}ALG2, ^{FLAG}ALG2, and ^{GFP}ALG2 and corresponding mutants were cloned into pEF-EntrA and recombined into pLentiX1-puro using Gateway LR clonase II (Invitrogen).

For expression in Sf9 ES insect cell expression, ^{His6x}Sec31A, ^{HA}Sec13, and ^{6xHis}MBP-Tev-PEF1 were cloned into pFastbac1 then recombined using the bac-to-bac baculovirus expression system (Invitrogen). ^{6xHisFLAG}ALG2 was cloned into pET28 for expression in *Escherichia coli.*

The following mutations were introduced into multiple vectors using site-directed mutagenesis of parental DNA followed by DpnI digestion: ALG2 E47A, E114A, F60A, and ΔEF5, PEF1 K137R, K165R, and K167R, KLHL12 FG289AA and LSE67AAA).

CRISPR/Cas9 guides were designed using the MIT CRISPR design tool and cloned into pLentiCRISPR v2 (a gift from Feng Zheng, addgene #52961). The sequences are as follows: PEF1 targeting, (GGAGCTGCAGGACAAGCACC), and ALG2 targeting, (GAACTCGCTGAAGTTCACGC), and non-targeting guide. Bacterial expression plasmids CUL3 purification and Nedd8 E1 (APPBP1-Uba3) were provided by Brenda Schulman (HHMI, St. Jude's Childrens Research Hospital).

siRNAs:

The following siRNA oligos were purchased from Dharmacon: Scrambled control (UAGCGACUAAACACAUCAAUU), PEF1 3'-UTR (GGUCCUUGUAAUGGAGUUAUU) ALG2 3'-UTR (CAUUGUGCCAUGAGGUAAAUU), KLHL12 SMARTpool (GGAAGGUGCCGGACUCGUAUU, GCAGGGAUCUGGUUGAUGAUU, GGACUAAUGUUACACCAAUUU, UGACAAAUACUCAUGCUAAUU), Lunapark SMARTpool (GAAACUUACAAGACGGCUAUU, GUGUUUACAUUAAGCGGUAUU, ACGAUGUUCUUGAUGAUAAUU, GUGGAACAGUUAAGUAGAAUU).

Antibodies

The following antibodies were used: KLHL12 (Cell Signaling, 9406, mouse monoclonal), KLHL12 (Novus, NB120-14233, chicken polyclonal), SEC31 (BD, 612350, mouse monoclonal), Sec31 (Santa Cruz, sc-376587, mouse monoclonal), PEF1/peflin (Abcam, ab137127, rabbit monoclonal), ALG2/PDCD6 (Proteintech, 12303-1-AP, rabbit polyclonal), CUL3 (Bethyl, A301-109A, rabbit polyclonal), Lunapark (Abcam, ab121416, rabbit polyclonal), pro-collagen I (QED, 42024, mouse monoclonal), GM130 (Abcam, ab52649 rabbit monoclonal) HA (Cell Signaling, C29F4, rabbit monoclonal), FLAG (Sigma, F7425, rabbit polyclonal,), β-actin (MP Biomedicals, clone 4, mouse monoclonal), GAPDH (Cell Signaling 14C10, rabbit monoclonal), α-tubulin (Calbiochem, DM1A, mouse monoclonal). SEC13 rabbit polyclonal antibody was a

gift from Randy Schekman at University of California Berkeley/HHMI. Goat-anti-Mouse Alexa488 and Goat-anti-Rabbit Alexa568 (Invitrogen), Donkey-anti-Chicken IgY Fluorescien (Jackson Immunoresearch), HRP Goat-anti-Mouse IgG light-chain specific (Jackson Immunoresearch), HRP Goat-anti-Mouse IgG (Sigma), and HRP Goat-anti-Rabbit IgG (Sigma) were used as secondary antibodies.

Recombinant Proteins

UbcH5, KLHL12, CUL3, and Nedd8 E1 were expressed and purified from BL21/DE3 (RIL) cells as described (Eletr et al., 2005; Jin et al., 2012). ^{6xHisFLAG}ALG2 was cloned into pET28 and grown to LB medium to OD^{600nm} 0.8 and induced with 0.5mM IPTG (Lab Scientific, Inc.) at 37°C for 3h. Cells were harvested at lysed by sonication in 20mM Tris (pH 8.0), 150mM NaCl with protease inhibitor tablets (Roche). Imidazole was added to 10mM and lysate was incubated with NiNTA resin (QIAGEN) for 2h at 4°C, and eluted in 20mM Tris (pH 8.0), 150mM NaCl, 300mM imidazole. Protein was diluted to 50µM and dialyzed overnight into 20mM Tris (pH 8.0), 150mM NaCal, 1mM DTT.

^{6xHis}Sec31A/Sec13 complex, Ube2M, and E1 were purified from Sf9 cells as described (Scott et al., 2011; Stagg et al., 2006; Wickliffe et al., 2011). PEF1 was also purified from Sf9 cells: ^{6xHis}MBP-TEV-PEF1 was cloned into pFastbac1, packaged into baculovirus, and expressed in Sf9 cells for 72h. Cells were collected and lysed by douncing in 50mM Tris (pH 8.0), 150mM NaCl with protease inhibitor. Imidazole was added to 10mM and lysate was incubated with NiNTA resin for 2h at 4°C. ^{6xHis}MBP-TEV-PEF1 was eluted with 50mM Tris (pH 8.0), 150mM NaCl, 300mM imidazole. Protein was dialyzed overnight into 50mM Tris (pH 8.0), 150mM NaCl. To obtain MBP-tagged protein, dialyzed protein at this step was used. To obtain untagged protein, dialyzed ^{6xHis}MBP-TEV-PEF1 was incubated overnight with ^{6xHis}TEV protease at 4°C. Cleaved ^{6xHis}MBP and ^{6xHis}TEV were removed by incubating with NiNTA resin.

Mammalian cell culture, transfections, and lentiviruses

Human embryonic kidney (HEK) 293T, Saos-2, and IMR90 cells were maintained in DMEM with 10% fetal bovine serum. HEK 293T cells expressing doxycycline-inducible $KLHL12^{FLAG}$ were grown in DMEM with certified Tet- fetal bovine serum. HT1080 cells expressing pro-collagen I and doxycycline-inducible $KLHL12^{FLAG}$ were grown in DMEM with 10% Tet- FBS with non-essential amino acids. Plasmid transfections of HEK 293T cells were with calcium phosphate or lipofectamine 2000 according to the manufacturers instructions, and siRNA transfections were with Lipofectamine RNAiMAX (Invitrogen) using 20nM for each siRNA.

Lentiviruses were produced in 293T cells by co-transfection of lentiviral constructs with packaging plasmids (Addgene) for 48–72h. Viruses were collected and filtered through a 0.45µm filter and stored at -80°C. Cells were transduced in polybrene (6µg/ml) and selected in puromycin (Sigma, 0.5-2µg/ml) until cell death was complete (2-7d).

Generating CRISPR/Cas9 knock-out cells

293T cells were transduced with lentiviruses containing Cas9 and sgRNA expression constructs (LentiCRISPR v2) and selected using puromycin for 7d. After selection, the degree of editing of the bulk cell population was determined by western blot for PEF1 and ALG2.

Microscopy
For immunofluorescence, cells were seeded on poly-d-lysine coated coverslips. Cells were fixed for 10min in 4% paraformaldehyde in PBS and washed three times in PBS. Cells were permeabilized in PBS with 0.1% Triton-X-100 for 10 minutes and blocked for 30min in PBS with 5% normal donkey serum. Cells were stained in primary antibody diluted in PBS for 2h at room temperature, washed 4 times in PBS, and incubated with fluorescent secondary antibodies and Hoechst (AnaSpec Inc.) for 45min at room temperature covered in foil. Coverslips were washed 4 times in PBS then mounted on glass slides using Pro-long gold antifade reagent (Life Technologies). For live cell imaging, cells were seeded on glass-bottom Lab-tek imaging chambers. Images were acquired on a Zeiss LSM 710 confocal microscope using 40X, 60X, and 100X oil objectives.

Large-scale immunoprecipitation-mass spectrometry and CompPASS analysis
αFLAG immunoprecipitations for mass spectrometry analysis were performed from extracts of HEK 293T cells transiently or virally expressing 1x-FLAG versions of KLHL12, Sec31A, PEF1, ALG2, and Lunapark (20 x 15cm dishes per condition). Cells were lysed in 2 pellet volumes of 50mM HEPES (pH 7.5), 1.5 mM MgCl2, 5mM KCl and 0.1% Triton-X100 by freeze//thaw in liquid nitrogen and multiple passages through a 25G5/8 needle. Debris was pelleted by centrifugation at 21000G for 1h, and lysates were passed through a 0.22µm filter for further clearing, then NaCl concentration was increased to 150mM. Under Ca^{2+} chelation conditions, EGTA was added at this step and in all future buffers to 5mM. Lysates were incubated with 100µl of αFLAG-M2 agarose resin (Sigma) for 2 h at 4°C, then beads were washed 5 times in cold 50mM HEPES (pH 7.5), 150mM NaCl,1.5 mM $MgCl_2$, 5mM KCl and 0.1% Triton-X100. Proteins were eluted in 3 incubation steps at 30°C each with 250µl of 3xFLAG peptide (0.5mg/ml in PBS). For sequential IPs, eluates were further incubated 100µl anti-HA-resin (SIGMA) for 2h at 4°C, washed 5 times as described above at eluted with 3xHA peptide (Biosynthesis). Eluates were processed for multi-dimensional protein identification technology (MuDPIT). CompPASS analysis was performed as described (Huttlin et al., 2015; Sowa et al., 2009).

Small-scale immunoprecipitation for Western analysis
Cells were collected and lysates were obtained as described above, with the exception of the 0.22µm filtration step, which was not performed for small-scale experiments. For FLAG IPs, lysates were incubated for 2h at 4°C with 15µl of αFLAG-M2 agarose, washed 5 times in cold HEPES (pH 7.5), 150mM NaCl,1.5 mM $MgCl_2$, 5mM KCl and 0.1% Triton-X100. For endogenous IPs, lysates were incubated for 2h at 4°C with 3µg of primary antibody, then coupled to 15µl Protein A/G fusion magnetic beads (ThermoFisher, #88803). Beads were washed 4 times and proteins were eluted in 2x sample buffer (25% glycerol, 3% SDS, 50mM Tris pH 6.8, 5% β-mercaptoethanol).

Vesicle size and number quantification
Doxycycline-inducible 293T::$KLHL12^{FLAG}$ cells were reverse-transfected with 20nM siRNA using Lipofectamine RNAiMAX and incubated for 48h on poly-lysine coated coverslips. Expression of $KLHL12^{FLAG}$ was induced by treatment with doxycycline (1µg/mL) for 12h. To assess knock-out cells, Control, PEF1, and ALG2 CRISPR-Cas9 knock-out cells were treated similarly. Cells were fixed for 10min in paraformaldehyde (4% in PBS) and processed for

immunofluorescence. KLHL12^{FLAG}-positive vesicles were determined by setting a pre-determined FLAG brightness threshold and using this to create binary Z-stack images using Metamorph. Vesicle number and size were then assessed by particle analysis in ImageJ. To assess response to Ca^{2+} influx, cells were processed as described above but treated for indicated amounts of time with ionomycin (3μM) in Ringers buffer.

Live cell imaging of calcium responses

Human embryonic kidney (HEK) 293T cells or IMR90 cells were infected with lentiviruses to express GFP-ALG2 WT and mutants. After 3 days, cells were seeded onto 8-well imaging chambers (Lab-Tek). For two-color movies, cells were transfected for 12hrs with RFP-Sec31A using lipofectamine 2000. Prior to imaging, cells were washed 2 times with Ringer's buffer or Ringer's buffer containing 10mM EGTA. Buffer was removed immediately prior to imaging and replaced with corresponding Ringer's buffers with DMSO, 3μM ionomycin (Sigma), or 10μM histamine (Sigma).

Calcium imaging

Ca^{2+} imaging experiments were carried out as previously described (Wilson et al., 2011). Cells were loaded for 30 min with 2 μM Fura-2AM, supplemented with 0.01% Pluronic F-127 (wt/vol, Life Technologies), in physiological Ringer's solution (in mM) 140 NaCl, 5 KCl, 10 HEPES, 2 $CaCl_2$, 2 $MgCl_2$ and 10 D-(+)-glucose, pH 7.4. EGTA solution contained: (in mM) 140 NaCl, 5 KCl, 10 HEPES, 10 EGTA 10 D-(+)-glucose, pH 7.4. Images were collected and analyzed using MetaFluor (Molecular Devices). Intracellular calcium concentration was determined from background-corrected F_{340}/F_{380} ratio images using the relation $[Ca^{2+}]_i = K^*(R-R_{min})/(R_{max}-R)$ (PMID: 3840439) with the following parameters measured in HEK293t cells: R_{min}=0.27; R_{max}=6.2; K^*=1.8mM. Image analysis and statistics were performed using custom routines in Igor Pro (WaveMetrics).

Collagen trafficking assays

Saos-2 cells were reverse transfected with siRNAs (20nM) and seeded onto coverslips in a 6-well dish. After 48h, cells were incubated for 3h at 40°C. After incubation, media was removed and replaced with DMEM with 10% fetal bovine serum, ascorbate (50μg/ml) and cycloheximide (50μg/ml) and temperature-shifted to 32°C. At indicated times, cells were fixed in 4% paraformaldehyde in PBS and processed for immunofluorescence.

Collagen retention assay

HT1080 cells expressing procollagen I and containing doxycycline-inducible KLHL12 were seeded into 35mm dishes at 150,000 cells per dish and reverse transfected with 20nM siRNAs targeting ALG2, PEF1, or both. 24h post-transfection, the medium was replaced with fresh DMEM/FBS and 20h later, the cells were induced with 2μg/mL doxycycline. The cells were harvested 12h post-induction, washed once with sterile PBS, and trypsinized. Trypsin was quenched with DMEM/FBS, the cells were spun down and washed once with sterile PBS. The washed cells were resuspended in 2X Laemmli/6M urea lysis buffer, sonicated, heated to 65°C, and the concentration of the total protein was determined by means of Pierce 660 protein assay. Equal amounts of total protein were resolved on SDS gel and analyzed by Western blotting for intracellular collagen.

Immunofluorescence imaging of calcium responses

293T cells expressing doxycycline-inducible KLHL12 were seeded on poly-lysine coated coverslips and reverse-transfected with siRNAs (20nM) when applicable. Prior to treatment, cells were washed twice with Ringer's buffer then incubated in Ringer's buffer with DMSO or 3μM ionomycin. Cells were fixed and processed for immunofluorescence.

Cellular ubiquitylation assays

For detection of SEC31A and PEF1 ubiquitylation, HEK293T cells were transfected with ^{6xHis}Ubiquitin and KLHL12^{FLAG}. To determine the effect of PEF1 and ALG2 depletion, cells with transfected with PEF1 and ALG2 siRNAs 24hrs before plasmid transfection. Cells were harvested washed with PBS, lysed in Urea lysis buffer (ULB) (8M urea, 300 mM NaCl, 0.5% NP40, 50 mM Na_2HPO_4, 50 mM Tris-HCl pH 8) and sonicated. ^{6xHis}Ubiquitin conjugates were purified by incubation and rotation with NiNTA agarose for 1h at room temperature. Beads were washed 5x with ULB supplemented with 10mM imidazole. Ubiquitin conjugated were eluted in sample buffer and ubiquitylated proteins were detected by western blot.

In vitro binding reactions

In vitro binding assays were performed at room temperature in binding buffer (150mM NaCl, 50mM KHEPES, pH 7.5, 3mg/mL BSA, 10% glycerol, 0.05% TWEEN, EDTA-free protease inhibitor tablets) supplemented either with 1mM EGTA or increasing CaCl2 concentrations (determined by fluorescence-based calcium imaging using Fura-2 ratiometric calcium-binding dye). Recombinant ^{6xHisFLAG}ALG2, PEF1, KHLH12, CUL3/RBX1 (1μM each) and 0.5μM SEC31 were mixed in the binding buffer and incubated at room temperature for 1h. The mixture was incubated with M2 anti-FLAG affinity resin (10μl) with mixing for 2h in a total volume of 90μl. The beads were washed six times with binding buffer and eluted with FLAG peptide in a total volume of 90μl by incubating at 30°C with mixing. 80μl of the eluted protein solution was mixed with 3X Laemmli buffer and heated for 5min at 95°C. The elution mixture was resolved on a denaturing gel and the protein levels were assayed by Western blotting. Similar experiments were performed to interrogate the association between ^{6xHisFLAG}ALG2 mutants (10μg) and SEC31/13 complexes, only that binding was assessed by SDS-PAGE and Coomassie staining.

PEF1 full length, N-terminal domain, and C-terminal domain were synthesized from pCS2+ vectors by *in vitro* transcription-translation in rabbit reticulocyte lysate (Promega). 1μg of DNA was combined with 20μl of rabbit reticulocyte lysate and 3μl of ^{35}S-labeled cysteine/methione mixture (Perkin Elmer). Reactions were incubated at 30°C for 2h. 10μg ^{MBP}KLHL12 (wt and FG289AA) was coupled to 20ul amylose resin (New England Biociences) in 50mM HEPES (pH 7.5), 150mM NaCl, 1.5 mM $MgCl_2$, 5mM KCl and 0.1% Tween20 for 1.5 h rotating at 4°C. Beads were washed 3 times in the same buffer, then 5μl *in vitro* translated PEF1 constructs were added. Reactions were incubated at 4°C for 2h, then washed 4 times. Proteins were eluted in sample buffer and detected by coomassie and autoradiography of SDS-PAGE gels.

***In vitro* ubiquitylation assays**

Ubiquitylation of SEC31 and PEF1 was performed using a modified reconstituted system as previously described (Jin et al., 2012). 5μM Cul3/Rbx1 was neddylated in the presence of 63μM Nedd8, 0.7μM E1, 0.8μM Ube2M, and energy regenerating system in 1X UBA buffer (50mM Tris-HCl pH 7.5, 50mM NaCl, 10mM $MgCl_2$) at 30°C for 7min. Recombinant KLHL12 was

added to neddylated Cul3/Rbx1 and diluted to 200nM Cul3/Rbx1, 330nM KLHL12). The ligase dilutions were mixed with the reaction mixture containing recombinant 50nM SEC31, 50nM PEF1, saturating ubiquitin, E1, UBCH5, energy regenerating system, and 100mM DTT in 1X UBA buffer. The reaction were carried out for 1h at 30°C and quenched with 2X Laemmli/6M urea. The samples were heated at 65°C and analyzed by Western blotting. If ubiquitylation of SEC31 was interrogated in the presence of PEF1 and ALG2, 50nM SEC31 was supplemented with 150nM PEF1 and 150nM ALG2. The reactions were performed for 1 h at 30°C and processed as described above. Competition between PEF1 and SEC31 ubiquitylation was assayed using 50nM SEC31 and increasing concentrations of Pef1 (0, 260, 520, 1040, 3420nM) and assayed in the presence of saturating ligase (550nM Cul3/Rbx1 and 1.59μM KLHL12).

In vivo Sec31-Alg2 ubiquitylation

HEK293T cells allowing for doxycycline inducible KLHL12 expression were transfected at 60% confluence with plasmids encoding ^{HIS6}ubiquitin, SEC13, ^{HA}SEC31 or the SEC31-ALG2 fusion using polyethyleneimine. 24h post-transfection, the cells were treated with 2μg/mL doxycycline and harversted 30h later. Cells were washed and the cell pellet was resuspened in 2mL of Urea lysis buffer (ULB) (8M urea, 300mM NaCl, 0.5% NP40, 50mM Na_2HPO_4, 50mM Tris-HCl, pH 8) and incubated on a rotary shaker for 20min. The samples were lysed by sonication, centrifuged at 15,000rpm, 15min, and the lysates were normalized for protein concentrations and adjusted to 2mL using ULB. Lysates were supplemented with 10mM imidazole, mixed with 300μl of Ni-NTA agarose, and incubated on a rotary shaker at room temperature for 1.5h. The resin was washed five times with 5mL per wash of ULB/10mM imidazole. The final wash was removed completely and the resin was resuspended in 250μl of 1X Laemmli buffer containing 300mM imidazole. The samples were incubated at 65°C with mixing for 10min, resolved on 10% and 5% denaturing gels, and analyzed by Western blotting. The CUL3-dependence of the SEC31-ALG2 fusion ubiquitylation was tested in cells co-transfected with dominant negative CUL3 (residues 1-252). The cells were treated and the samples processed as described above.

Figures

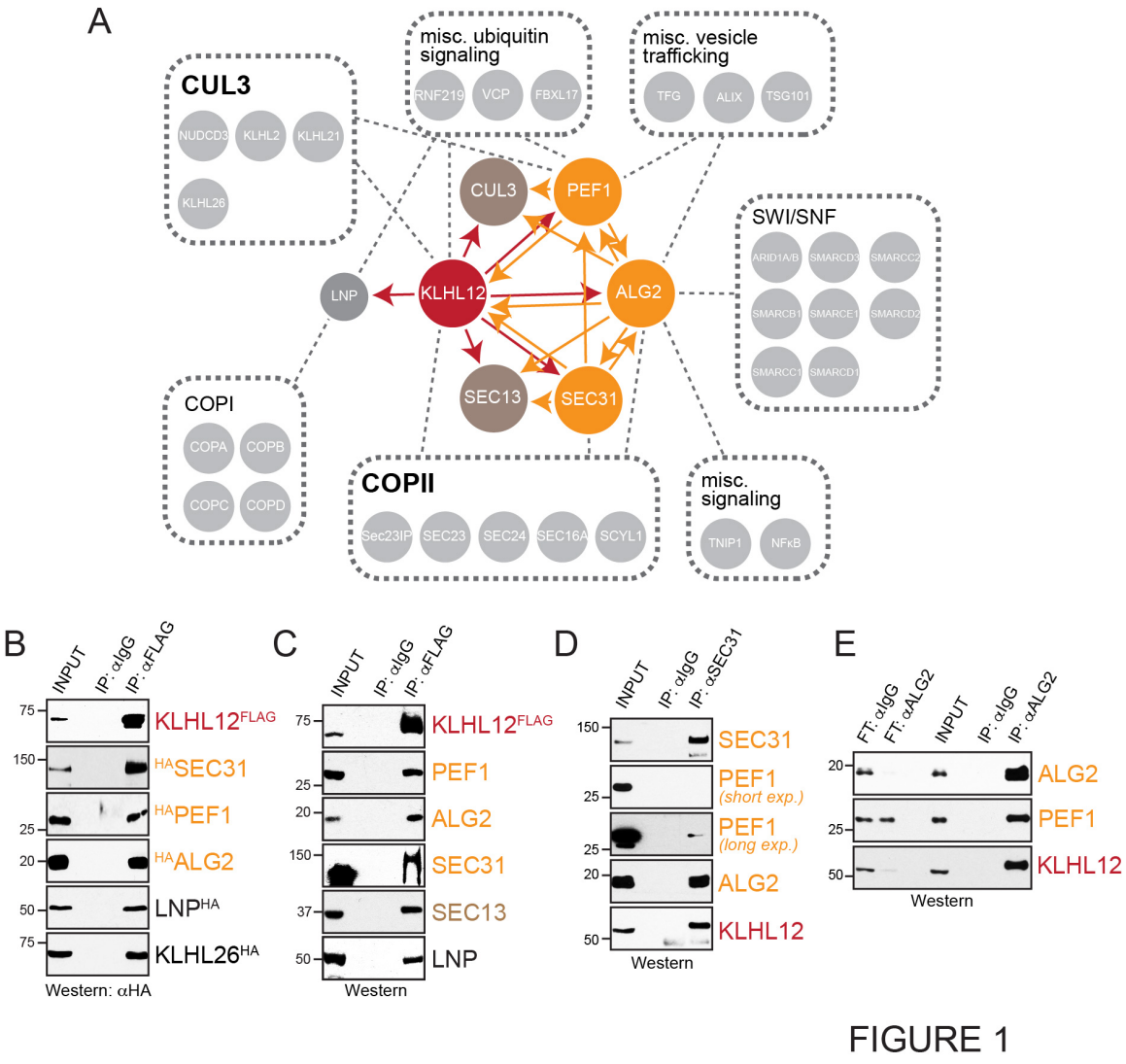

FIGURE 1

Figure 1: PEF1 and ALG2 bind CUL3^{KLHL12}. A. Graphical depiction of the protein interaction network centered on CUL3^{KLHL12} and SEC31. Proteins marked with red (KLHL12) or orange (PEF1, ALG2, SEC31) dots were used as baits for affinity-purification coupled to CompPASS mass spectrometry, and specific binding partners are shown. Total spectral counts for representative experiments are depicted in Figure S1. **B.** Validation of proteomic experiments by αFLAG-affinity-purification coupled to Western blotting, using KLHL12^{FLAG} and selected HA-tagged high-confidence interactors of KLHL12. **C.** Validation of proteomic experiments by αFLAG-affinity-purification coupled to Western blotting, using specific antibodies to detect endogenous high-confidence interactors of ^{FLAG}KLHL12. **D.** PEF1, ALG2, and KLHL12 associate with SEC31. Endogenous SEC31 was affinity-purified using specific αSEC31-antibodies, and co-purifying endogenous proteins were determined by Western blotting. **E.** ALG2 efficiently binds PEF1 and KLHL12. Endogenous ALG2 was affinity-purified using αALG2-antibodies and co-purifying PEF1 and KLHL12 were detected by Western blotting. The left side of the blots shows the supernatant of the immunoprecipitation experiments. Depletion of ALG2 from cell lysates results in co-depletion of KLHL12, underscoring the efficient nature of this interaction.

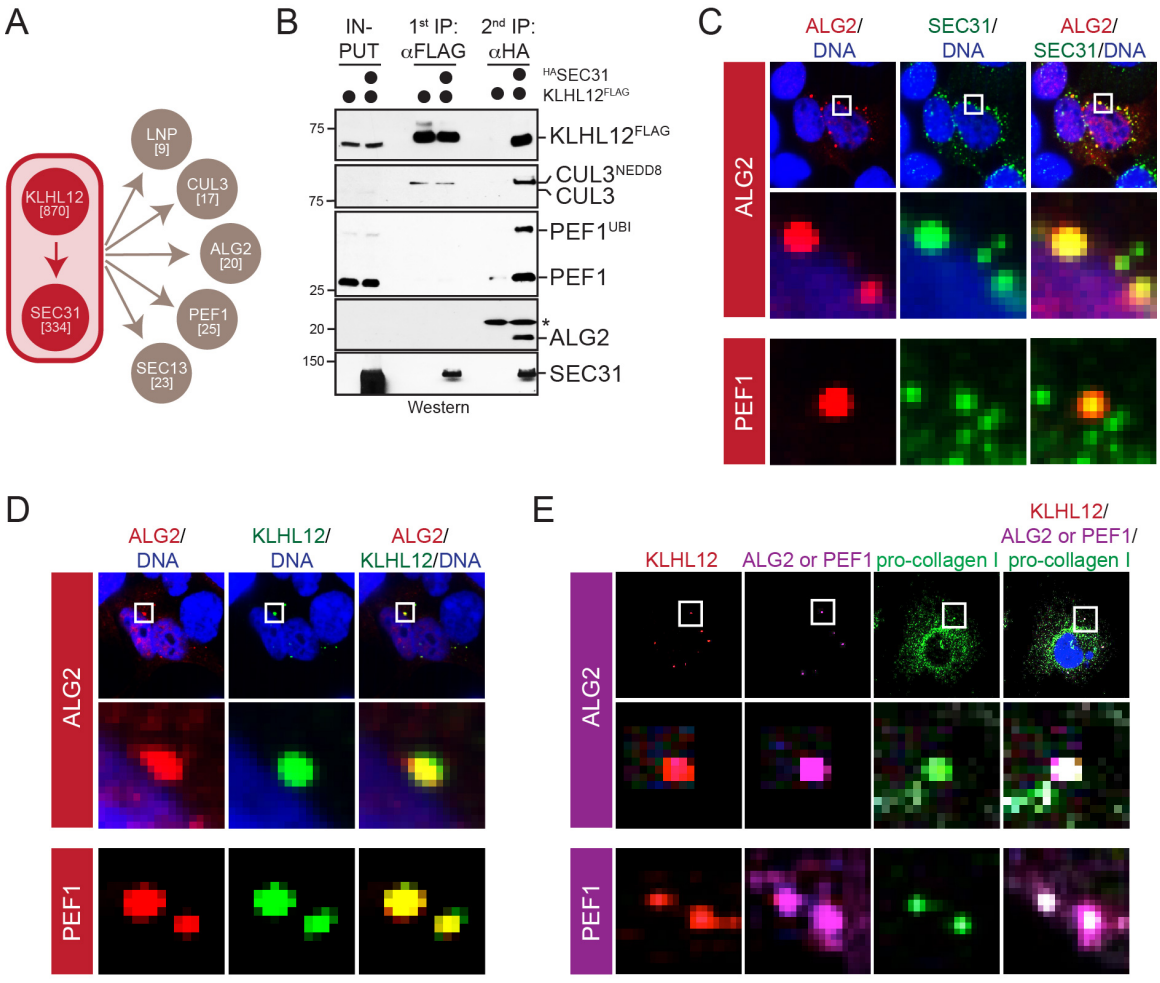

FIGURE 2

Figure 2: PEF1 and ALG2 associate with growing COPII coats. A. PEF1 and ALG2 stably bind KLHL12-SEC31 complexes. KLHL12-SEC31 complexes were isolated by sequential affinity-purification, and bound proteins were determined by CompPASS mass spectrometry. Specific high-confidence interactors and total spectral counts are shown. **B.** Validation of proteomic analysis of sequential KLHL12-SEC31 affinity-purification by Western blotting, testing for endogenous high-confidence interactors. Both PEF1 and ALG2 are enriched in affinity-purifications, indicative of a stable interaction with KLHL12-SEC31 complexes. **C.** PEF1 and ALG2 localize with SEC31 on large COPII coats. Cells expressing KLHL12 were stained for SEC31 (green), DNA (blue), and $PEF1^{HA}$ or $^{HA}ALG2$ (red), respectively. **D.** PEF1 and ALG2 co-localize with KLHL12. Cells expressing KLHL12 were stained for $KLHL12^{FLAG}$ (green), DNA (blue), and $PEF1^{HA}$ or $^{HA}ALG2$ (red), respectively. **E.** PEF1 and ALG2 localize with KLHL12 to collagen-I carriers. HT1080 cells expressing collagen-I were stained for $KLHL12^{FLAG}$ (red), $^{HA}ALG2$ or $PEF1^{HA}$ (purple), collagen-I (green) and DNA (blue).

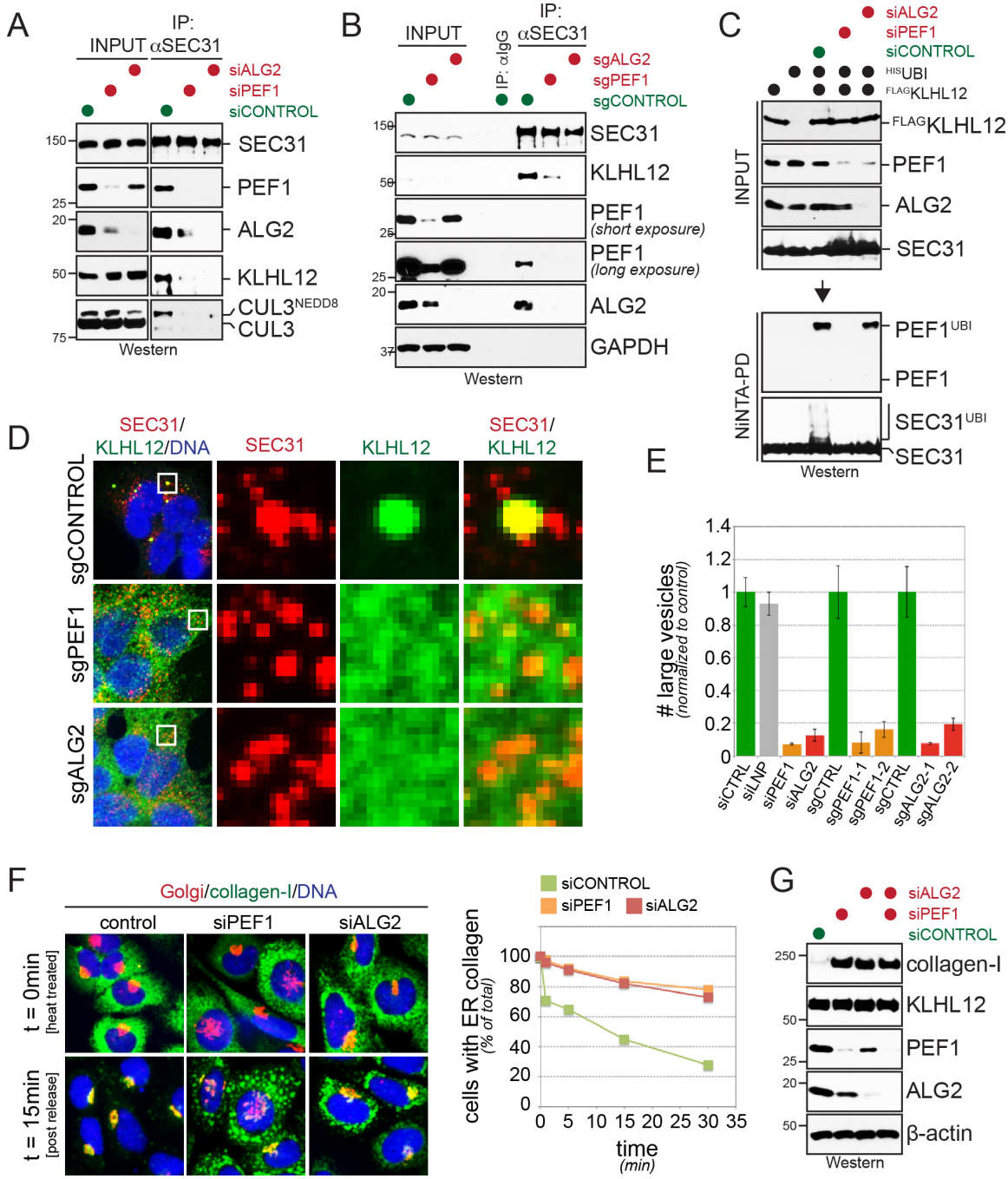
A
IP:
INPUT αSEC31
siALG2
siPEF1
siCONTROL
150
SEC31
PEF1
25
20
ALG2
50
KLHL12
CUL3NEDD8
CUL3
75
Western
B
INPUT
IP: αIgG
IP:
αSEC31
sgALG2
sgPEF1
sgCONTROL
150
SEC31
50
KLHL12
PEF1
(short exposure)
25
PEF1
(long exposure)
25
20
ALG2
37
GAPDH
Western
C
siALG2
siPEF1
siCONTROL
HISUBI
FLAGKLHL12
INPUT
FLAGKLHL12
PEF1
ALG2
SEC31
PEF1UBI
PEF1
NiNTA-PD
SEC31UBI
SEC31
Western
D
SEC31/
KLHL12/DNA
SEC31
KLHL12
SEC31/
KLHL12
sgCONTROL
sgPEF1
sgALG2
E
large vesicles
(normalized to control)
1.4
1.2
1
0.8
0.6
0.4
0.2
0
siCTRL
siLNP
siPEF1
siALG2
sgCTRL
sgPEF1-1
sgPEF1-2
sgCTRL
sgALG2-1
sgALG2-2
F
Golgi/collagen-I/DNA
control
siPEF1
siALG2
t = 0min
[heat treated]
t = 15min
[post release]
siCONTROL
siPEF1
siALG2
cells with ER collagen
(% of total)
100
80
60
40
20
0
0 5 10 15 20 25 30 35
time
(min)
G
siALG2
siPEF1
siCONTROL
250
collagen-I
KLHL12
50
PEF1
25
20
ALG2
50
β-actin
Western

FIGURE 3

Figure 3: PEF1 and ALG2 are required for CUL3^{KLHL12} activation. A. PEF1 and ALG2 are required for substrate recognition by CUL3^{KLHL12}. Human embryonic kidney cells were depleted of PEF1 or ALG2, and endogenous SEC31 was affinity-purified using specific antibodies. Co-precipitating proteins were detected by Western blotting. **B.** PEF1 and ALG2 are required for substrate recognition by CUL3^{KLHL12}, as determined after CRISPR/Cas9-based genome editing. Human embryonic kidney cells were transduced with sgRNAs targeting *PEF1* and *ALG2*, and endogenous SEC31 was purified as described above. Co-precipitating proteins were detected by Western blotting. **C.** PEF1 and ALG2 are required for SEC31 ubiquitylation in cells. ^{FLAG}KLHL12 was induced in ^{HIS}ubiquitin expressing human embryonic cancer cells, and ubiquitylated proteins were purified by denaturing NiNTA-pulldown and analyzed by Western blotting. **D.** PEF1 and ALG2 are required for the CUL3^{KLHL12}-dependent increase in COPII coat size. Expression of KLHL12 was induced in human embryonic cancer cells that were transduced with control sgRNAs or sgRNAs targeting PEF1 or ALG2. Formation of large COPII coats was monitored by SEC31 and KLHL12 co-localization using indirect immunofluorescence microscopy. **E.** Quantification of multiple experiments measuring CUL3^{KLHL12}-dependent formation of large COPII coats in the presence of different siRNAs or sgRNAs targeting PEF1 or ALG2. **F.** PEF1 and ALG2 drive collagen secretion. Human SaOS2 osteosarcoma cells were pulsed at 40°C to retain collagen-I in the ER. Cells were then shifted to 32°C to allow for synchronous export of endogenous collagen-I from the ER to the Golgi apparatus. ER exit of collagen was monitored over time by indirect immunofluorescence microscopy (*left panel*) and number of cells with ER-resident collagen-I was quantified (*right panel*). **G.** PEF1 and ALG2 support collagen secretion from cells. HT1080 cells stably expressing collagen-I were analyzed for intracellular retention of collagen-I in the presence of either control siRNAs or siRNAs targeting PEF1 and/or ALG2.

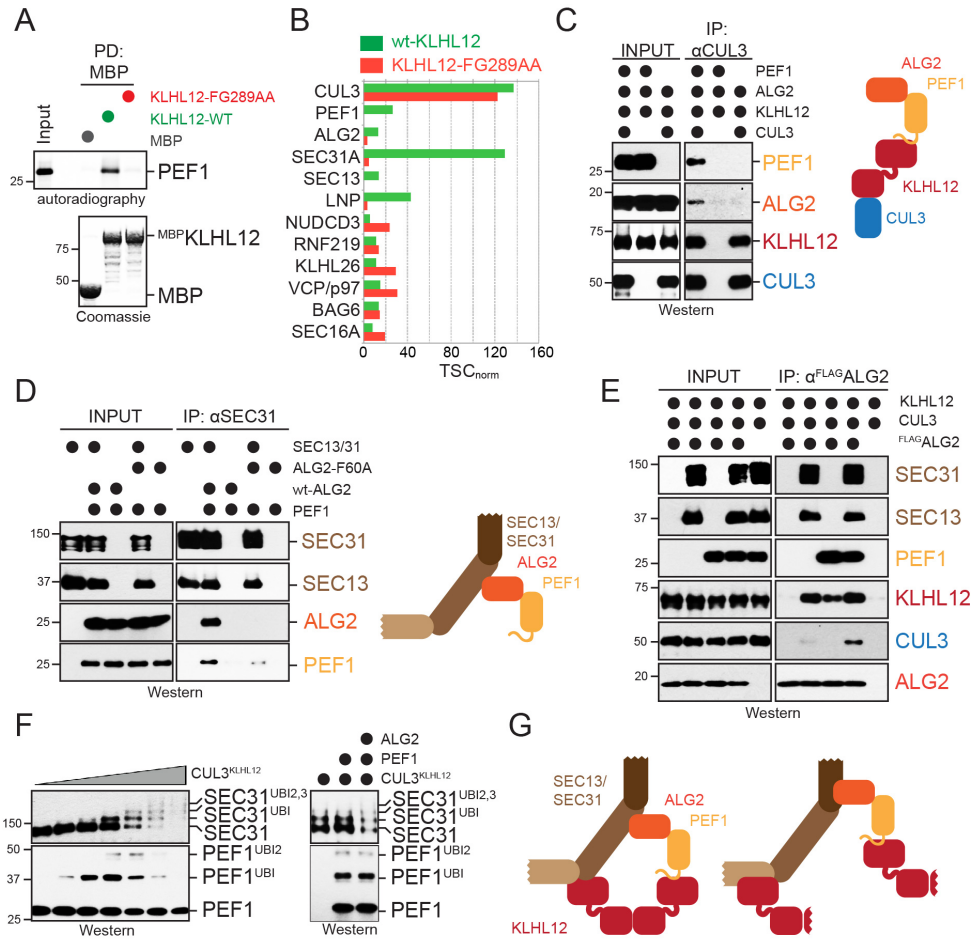

FIGURE 4

Figure 4: PEF1 and ALG2 form a target-specific co-adaptor for CUL3^{KLHL12}. A. PEF1 binds to the substrate-binding surface in the Kelch repeat of KLHL12. MBP, ^{MBP}KLHL12, or substrate-binding deficient ^{MBP}KLHL12^{FG289AA} were immobilized on beads and incubated with ^{35}S-labeled PEF1. Bound PEF1 was detected by autoradiography. **B.** PEF1 binds to the substrate-binding surface of KLHL12 in cells. FLAG-epitope tagged KLHL12 or KLHL12^{FG289AA} were affinity-purified from cells and analyzed for bound proteins by CompPASS mass spectrometry. Normalized total spectral counts for both proteomic experiments are shown. **C.** PEF1 bridges an interaction between KLHL12 and ALG2. Binding of recombinant ALG2 to immobilized CUL3^{KLHL12} was analyzed in the presence or absence of recombinant PEF1. The reactions were performed in the presence of human cell lysate, which reduced non-specific precipitation of PEF1. **D.** ALG2 mediates an interaction between PEF1 and SEC31. Binding of recombinant PEF1 to SEC31/13 complexes was analyzed in the presence of either wild-type ALG2 or ALG2^{F60A} (a mutant of ALG2 with reduced affinity for SEC31). **E.** SEC31 and PEF1 can both mediate binding of ALG2 to KLHL12. Binding of ALG2 to CUL3^{KLHL12} was analyzed in the presence of SEC31/13, PEF1, or both. **F.** PEF1 and ALG2 slightly stimulated SEC31 ubiquitylation by CUL3^{KLHL12} in vitro. *Left panel:* titration of CUL3^{KLHL12} shows dose-dependent ubiquitylation and turnover of SEC31. *Right panel*: addition of PEF1-ALG2 complexes to CUL3^{KLHL12} in vitro ubiquitylation reactions stimulates SEC31 modification. **G.** Proposed architecture of the CUL3^{KLHL12}-PEF1-ALG2-SEC31 complex (two possible arrangements are shown).

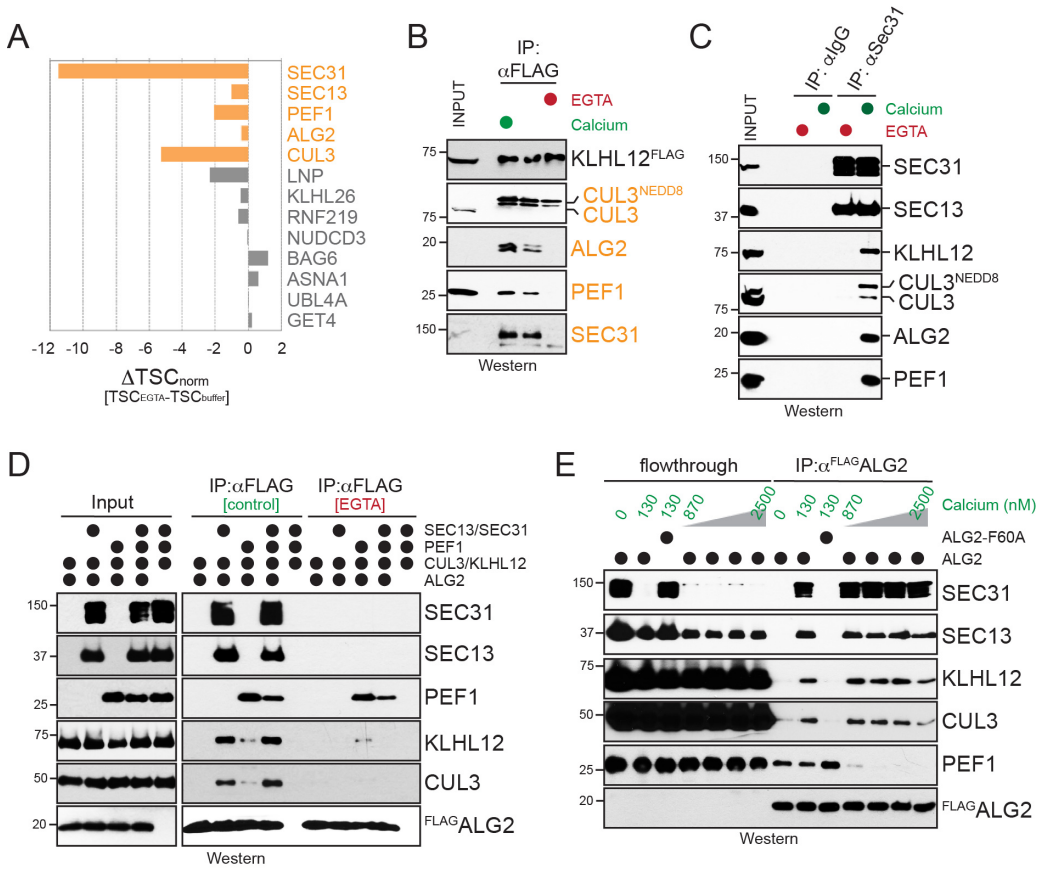

FIGURE 5

Figure 5: PEF1 and ALG2 impose calcium-regulation on CUL3^{KLHL12}. A. Calcium chelation reduces binding of KLHL12 to SEC31/13, CUL3, PEF1, ALG2, and Lunapark, but does not affect other interactions of KLHL12. KLHL12^{FLAG} was purified from cell lysates that were treated with EGTA, and bound proteins were identified by CompPASS mass spectrometry. Comparison of normalized total spectral counts to control immunoprecipitations is shown. **B.** Calcium is required for substrate recognition of CUL3^{KLHL12}. KLHL12^{FLAG} was precipitated from cell lysates either in the presence or absence of EGTA, and bound proteins were detected by Western blotting using specific antibodies. **C.** Calcium is required for substrate recognition of endogenous CUL3^{KLHL12}. SEC31 was precipitated from cell lysates treated with EGTA using specific antibodies, and endogenous proteins associated with SEC31 were determined by Western blotting. **D.** Calcium is required for formation of CUL3^{KLHL12}-PEF1-ALG2-SEC31 complexes in vitro. ^{FLAG}ALG2 was incubated with the indicated combinations of recombinant proteins either in the presence (control) or absence (EGTA) or calcium. Complexes containing ^{FLAG}ALG2 were then immobilized on αFLAG-resin and analyzed for bound proteins by Western. CUL3 was expressed as a split protein, with only the 50kD fragment being detected by the antibody. **E.** Physiologically relevant calcium concentrations support formation of CUL3^{KLHL12}-PEF1-ALG2-SEC31 complexes in vitro. ^{FLAG}ALG2 or ^{FLAG}ALG2^{F60A} (a calcium-signaling deficient variant of ALG2) were immobilized on FLAG-agarose and incubated with the indicated proteins at either 10mM EGTA; 130nM calcium (to mimic the cellular concentration seen upon calcium release from the ER); or 800nM calcium and above.

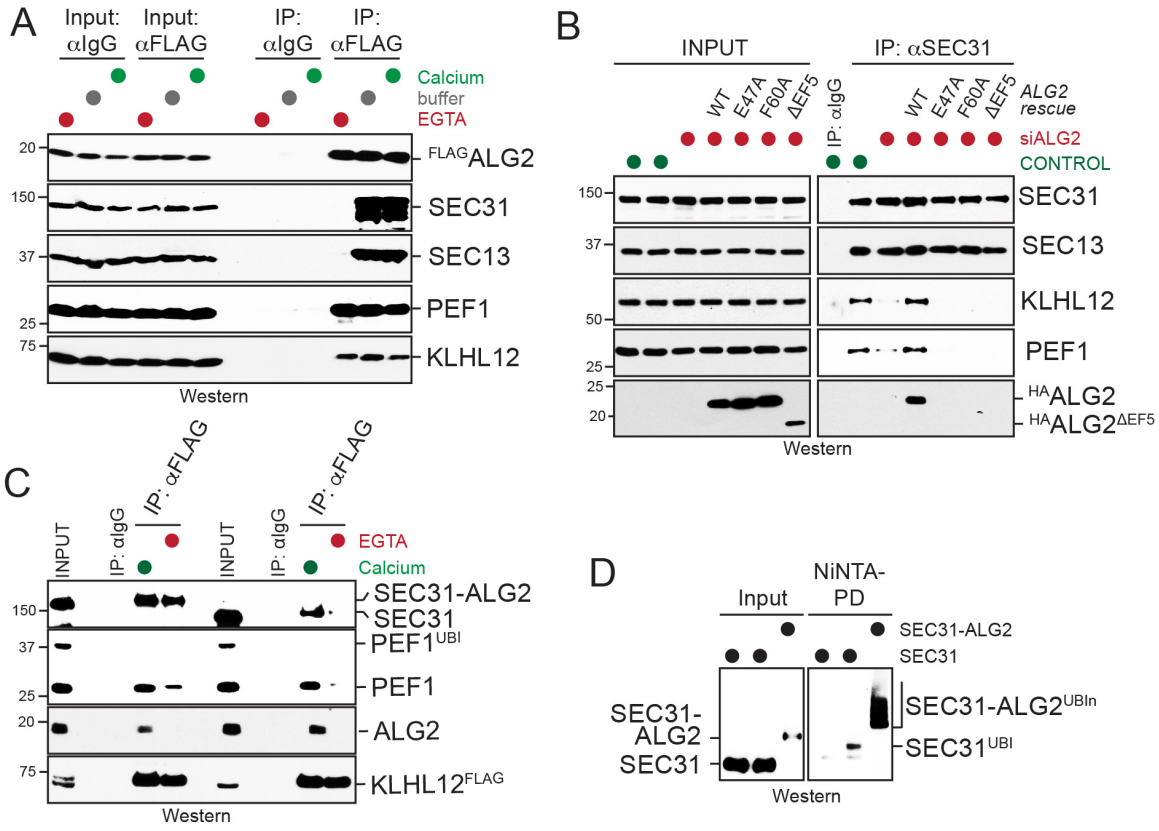

FIGURE 6

Figure 6: Calcium binding to ALG2 is required and sufficient for substrate recognition by CUL3^{KLHL12}. A. Calcium chelation inhibits association of ALG2 with SEC31, but not PEF1 and ALG2. Cell lysates were treated with EGTA to chelate calcium or additional $CaCl_2$, ^{FLAG}ALG2 was purified, and bound endogenous proteins were detected by Western blotting. **B.** Calcium-binding to ALG2 is required for substrate recognition by CUL3^{KLHL12}. Cells were depleted of endogenous ALG2 using specific siRNAs. Following expression of siRNA-resistant wild-type ALG2, ALG2^{E47A} (deficient in calcium-binding), ALG2^{F60A} (mutant hydrophobic surface exposed upon calcium binding), or ALG2$^{\Delta EF5}$ (deficient in binding to PEF1 and thus, defective integration into CUL3^{KLHL12}), endogenous SEC31 was affinity purified. Bound proteins were detected by Western blotting. **C.** Calcium-binding to ALG2 is sufficient for substrate recognition by CUL3^{KLHL12}. ALG2 and SEC31 were fused to establish a persistent, rather than dynamic calcium-dependent, interaction. The fusion protein was purified from cell lysates that were treated with either $CaCl_2$ or EGTA, as indicated, and bound proteins were detected by Western blotting. **D.** Dynamic substrate recognition ensures monoubiquitylation. ^{FLAG}SEC31 or the ^{FLAG}SEC31-ALG2 fusion were purified from cells expressing ^{HIS}ubiquitin under denaturing conditions and tested for ubiquitylation by αFLAG-Western blotting.

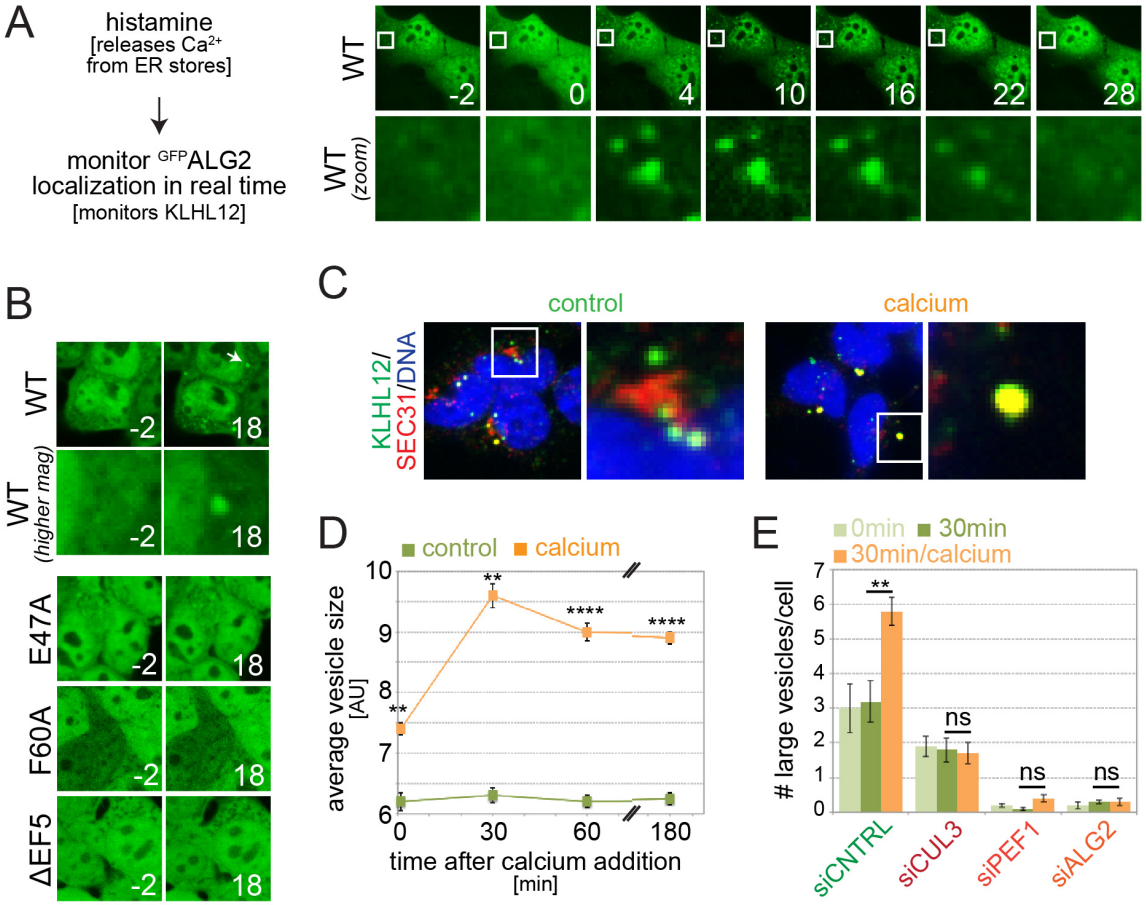

FIGURE 7

Figure 7: Regulated activation of CUL3^{KLHL12} allows for calcium-dependent control of COPII coat size. A. Release of calcium from the ER triggers relocalization of ^{GFP}ALG2 to vesicles. Immortalized human IMR90 cancer cells were treated with histamine, which results in opening of ER-resident calcium channels. Localization of ^{GFP}ALG2 was then followed by live-cell imaging. **B.** Increasing cytosolic calcium levels recruit ^{GFP}ALG2 to vesicles dependent on its ability to bind SEC31 and CUL3^{KLHL12}-PEF1. Localization of ^{GFP}ALG2, ^{GFP}ALG2^{E47A} (unable to bind calcium and SEC31), ^{GFP}ALG2^{F60A} (unable to undergo a calcium-dependent conformational change required to bind SEC31), and ^{GFP}ALG2$^{\Delta EF5}$ (unable to bind PEF1) was analyzed after calcium influx using live cell imaging. Only wild-type ^{GFP}ALG2 redistributed to vesicular structures following an increase in cytosolic calcium levels. **C.** Calcium induces an increase in COPII coat size. Human embryonic kidney cells expressing KLHL12 were exposed to higher cytosolic calcium levels, and the size of KLHL12-positive COPII coats was monitored by indirect immunofluorescence microscopy. **D.** Images as described in Figure 7C were subjected to automated image analysis and the average COPII coat size was determined as a function of the time after calcium influx into cells. **E.** Ubiquitin- and calcium-dependent regulation of COPII coat size. Human embryonic kidney cells expressing KLHL12 were depleted of CUL3, PEF1, or ALG2, as indicated. After calcium influx was triggered, the number of large KLHL12-positive vesicles was measured using automated image analysis.

bait: / binder:	KLHL12 (1644)	SEC31 (5461)	PEF1 (472)	ALG2 (524)	LNP (395)	KLHL12/ SEC31/
KLHL12		17	131	11	41	870
SEC31	210			419		345
PEF1	43	13		263		25
ALG2	22	11	29			20
LNP	71					9
Ub	62	8	191	26	17	26
CUL3	225	4	94	94	24	17
SEC13	23	566		148		23
SEC16A	14		14	89	16	89
NUDCD3	10		11		3	
FBXL17	20		6			
RNF219	20				28	
KLHL26	19		10			3
CUL1	10					
BAG6	28		7			
SEC23B	3	8				
SEC23A	4	25	4	2		
SCYL1		377				
SEC23IP		439		82		
SEC24C		38			6	
SEC24D		6				
P4HB			152			
P4HA1			109	33		
PPM1A			31			
FASN			77		89	
ARIH1			13			
SMARCB1				58		
PDCD6IP				687		
DPF2				53		
HEBP2				307		
SMARCD1				58		
TFG				30	6	
SMARCC1				181		
KCTD15				15		
NFkB p105				56		
ARID1A				153		
TNIP1				22		
SMARCE1				48		
CHERP				49		
TSG101				13		
FAM125A				13		
SMARCC2				63		
ARID1B				43		
SMARCA2				56		
SEC24B				9		
VCP					81	
COPA					59	
COPB					22	
COPC					33	
COPD					12	
COPB					22	

FIGURE S1

Figure S1: Interaction network of the CUL3^{KLHL12} ubiquitin ligase. High-confidence interactors of KLHL12, SEC31, PEF1, and ALG2 were determined by affinity-purification coupled to CompPASS mass spectrometry. Peptide counts for high confidence interactors are shown. The last column shows the results of a sequential affinity-purification of KLHL12-SEC31 complexes.

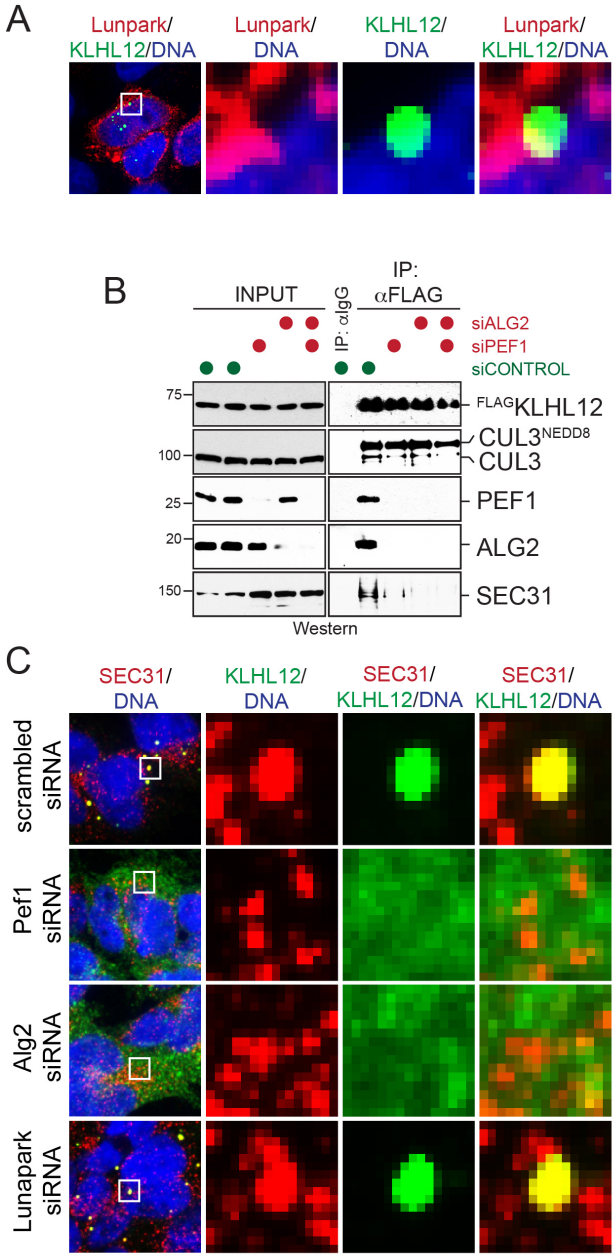

FIGURE S2

Figure S2: PEF1 and ALG2 are required for substrate binding by CUL3^{KLHL12}. A. Lunapark does not co-localize with KLHL12 on large COPII coats. Cells expressing both Lunapark^{HA} and KLHL12^{FLAG} were analyzed for protein localization using indirect immunofluorescence microscopy. **B.** PEF1 and ALG2 are required for substrate binding by CUL3^{KLHL12}. KLHL12^{FLAG} expressing cells were transfected with control siRNAs or siRNAs targeting PEF1 or ALG2. KLHL12 was immunoprecipitated on αFLAG-agarose, and bound proteins were analyzed by Western blotting. **C.** PEF1 and ALG2, but not Lunapark, are required for formation of large COPII coats. KLHL12-expressing cells were transfected with control siRNAs or siRNAs targeting PEF1, ALG2, or Lunapark, and analyzed for SEC31 and KLHL12 co-localization by indirect immunofluorescence microscopy.

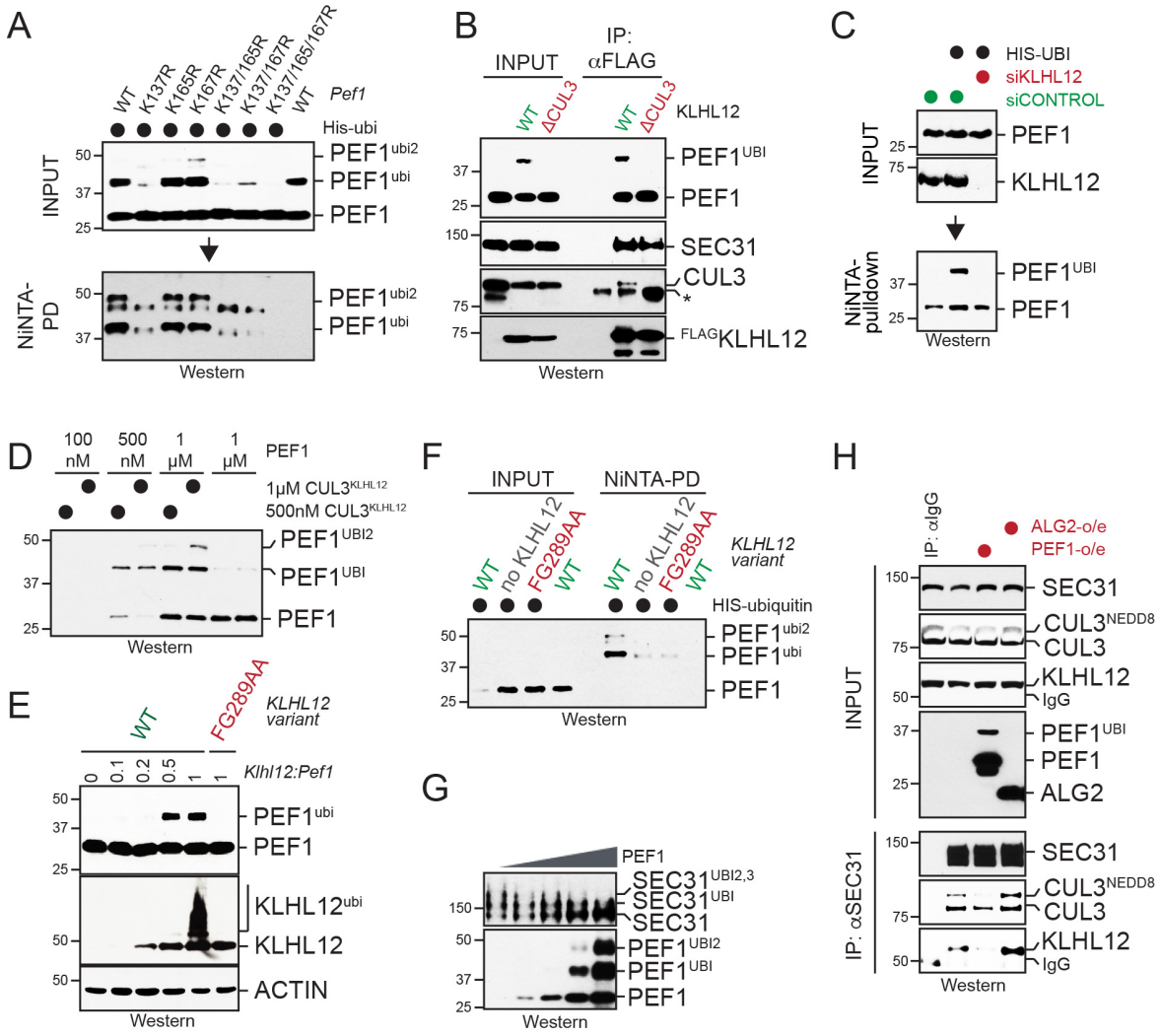

FIGURE S3

Figure S3: PEF1 binds the Kelch repeats of KLHL12. A. PEF1 is ubiquitylated in cells. PEF1 or variants of PEF1 with mutations in indicated Lys residues were expressed in cells that also produced ^{HIS}ubiquitin. Ubiquitylated proteins were purified under denaturing conditions on NiNTA agarose and analyzed for modified PEF1 by Western blotting. **B.** CUL3^{KLHL12} ubiquitylates PEF1 in cells. FLAG-epitope tagged KLHL12 or KLHL12$^{\Delta CUL3}$ (a variant unable to associate with CUL3) were affinity-purified from human embryonic kidney cells and analyzed for bound proteins by Western blotting. Expression of KLHL12, but not KLHL12$^{\Delta CUL3}$, induced monoubiquitylation of PEF1. **C.** Endogenous CUL3^{KLHL12} ubiquitylates endogenous PEF1. Cells expressing ^{HIS}ubiquitin were transfected with siRNAs targeting KLHL12. Ubiquitylated proteins were purified under denaturing conditions and tested for PEF1 modification by Western blotting. **D.** CUL3^{KLHL12} ubiquitylates PEF1 in vitro. Increasing concentrations of recombinant PEF1 were incubated with either 0.5μM or 1μM recombinant CUL3^{KLHL12}, E1, UBE2D3, ubiquitin, and ATP. Ubiquitylation of PEF1 was analyzed by Western blotting. **E.** CUL3^{KLHL12} ubiquitylates PEF1 in cells. Cells were transfected with increasing amounts of KLHL12 or substrate-binding deficient KLHL12^{FG289AA}, and ubiquitylation of PEF1 was analyzed by Western blotting. **F.** CUL3^{KLHL12} ubiquitylates PEF1 in cells. ^{HIS}ubiquitin-expressing cells were transfected with KLHL12 or substrate-binding deficient KLHL12^{FG289AA}. Ubiquitylated proteins were purified under denaturing

conditions over NiNTA agarose and analyzed for PEF1 by Western blotting. **G.** PEF1 and SEC31 compete for access to KLHL12. In vitro ubiquitylation reactions of recombinant SEC31 (in complex with SEC13) were performed by $CUL3^{KLHL12}$, E1, UBE2D3, and ATP in the presence of increasing PEF1 concentrations. SEC31 and PEF1 ubiquitylation was detected by Western blotting. **H.** SEC31 and PEF1 compete for access to KLHL12 in cells. Endogenous SEC31 was affinity-purified from cells that overexpressed either PEF1 or ALG2, and bound $CUL3^{KLHL12}$ was detected by Western blotting.

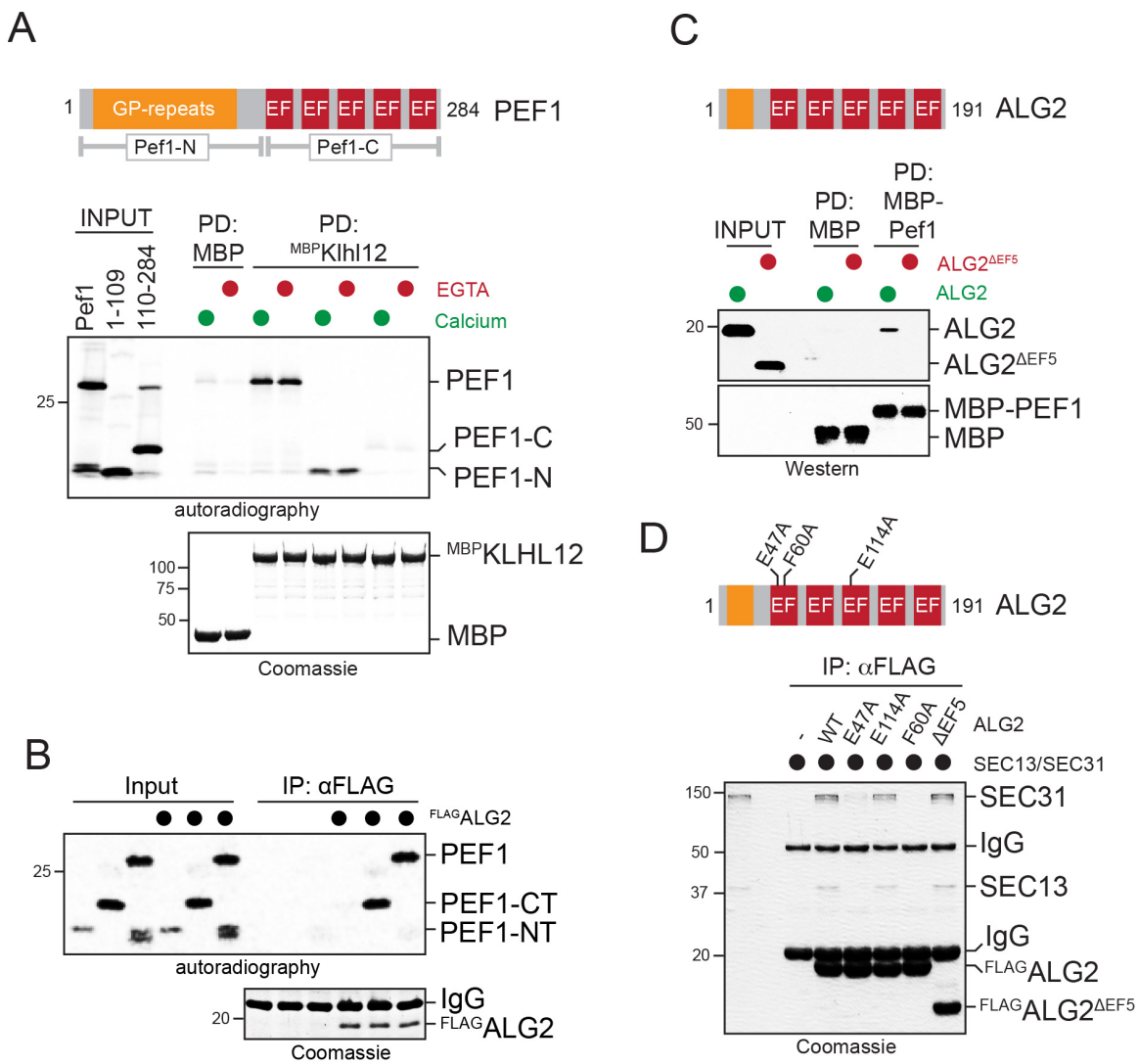

FIGURE S4

Figure S4: Architecture of the CUL3^{KLHL12}-PEF1-ALG2-SEC31 complex. A. PEF1 binds KLHL12 through its amino-terminal Gly-Pro repeats. ^{35}S-labeled PEF1, N-PEF1 (i.e. Gly-Pro-rich repeats), or PEF1-C (EF-hand domains) were incubated with immobilized MBP or ^{MBP}KLHL12, respectively. Bound PEF1 proteins were detected by autoradiography. **B.** PEF1 binds ALG2 through its carboxy-terminal EF hand domain. ^{35}S-labeled PEF1 proteins (described above) were incubated with immobilized ^{FLAG}ALG2, and bound proteins were detected by autoradiography. **C.** ALG2 binds to PEF1 through its fifth EF hand. Recombinant ALG2 or ALG2$^{\Delta EF5}$ were incubated with immobilized MBP or ^{MBP}PEF1, respectively. Bound proteins were detected by Western blotting. **D.** ALG2 binds SEC31 through its first EF hand. Recombinant SEC31 was incubated with immobilized wild-type ALG2 or variants of ALG2 with mutations in the 1st EF hand (E47A, F60), 3rd EF hand (E114A), or 5th EF hand (ΔEF5). Bound proteins were detected by Coomassie staining.

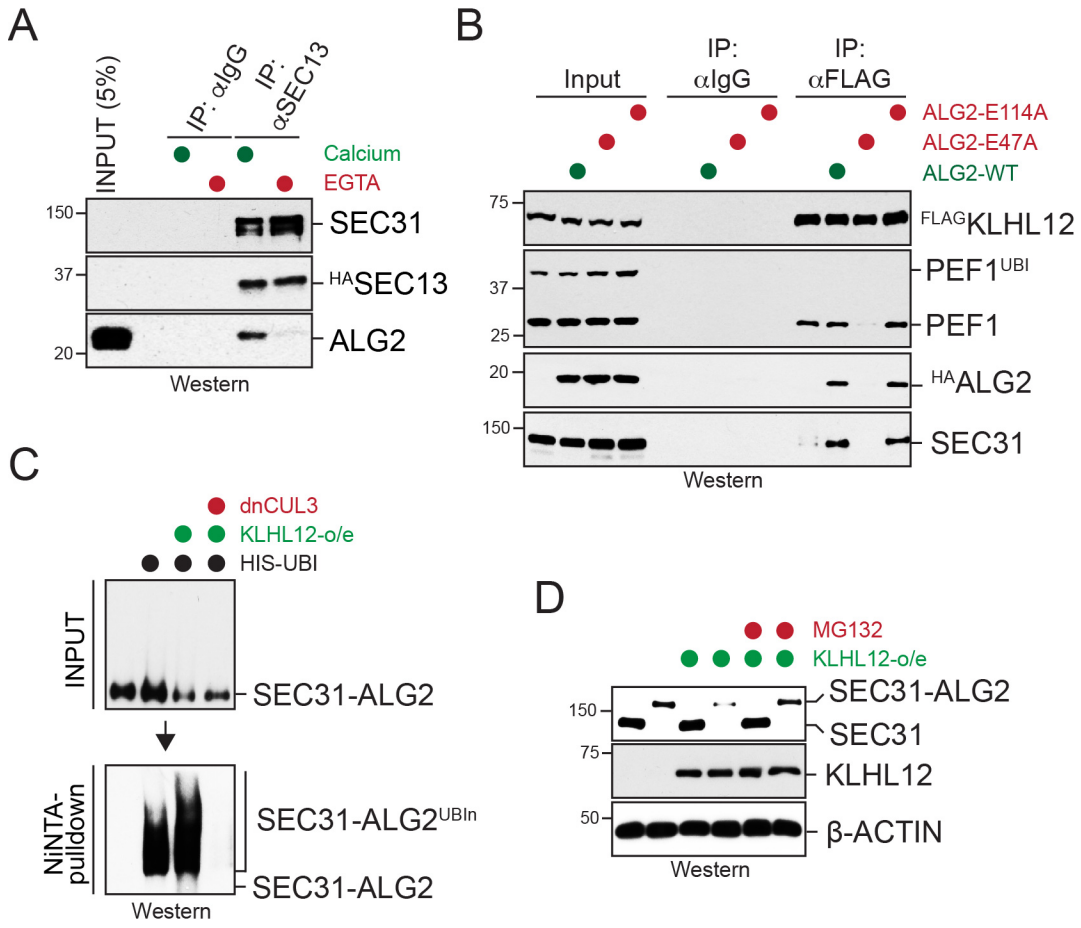

FIGURE S5

Figure S5: CUL3^{KLHL12} is a calcium-dependent ubiquitin ligase. A. Chelation of calcium abrogates the interaction between SEC31 and ALG2. Recombinant SEC31 was immobilized on beads using αHA antibodies, incubated with ALG2, and analyzed for bound proteins by Western blotting. Experiments were performed in the presence or absence (EGTA) of calcium. **B.** Calcium-binding deficient ALG2^{E47A} disrupts formation of the CUL3^{KLHL12} ubiquitin ligase. KLHL12 was immunoprecipitated from control cells or from cells that overexpressed wild-type ALG2, ALG2^{E47A}, or ALG2^{E114A}. Bound proteins were detected by Western blotting. **C.** CUL3^{KLHL12} ubiquitylates the SEC31-ALG2 fusion protein. The SEC31-ALG2 fusion was expressed in human embryonic kidney cells that also produced ^{HIS}ubiquitin. KLHL12 and dominant negative CUL3$^{1-252}$ were expressed as indicated. Ubiquitylated proteins were purified under denaturing conditions over NiNTA agarose, and analyzed for SEC31-ALG2 modification using Western blotting. **D.** Polyubiquitylation of the SEC31-ALG2 fusion triggers its proteasomal degradation. Cells were transfected with SEC31, SEC31-ALG2, and KLHL12 as indicated. When noted, cells were treated with the proteasome inhibitor MG132, and protein levels were determined by Western blotting.

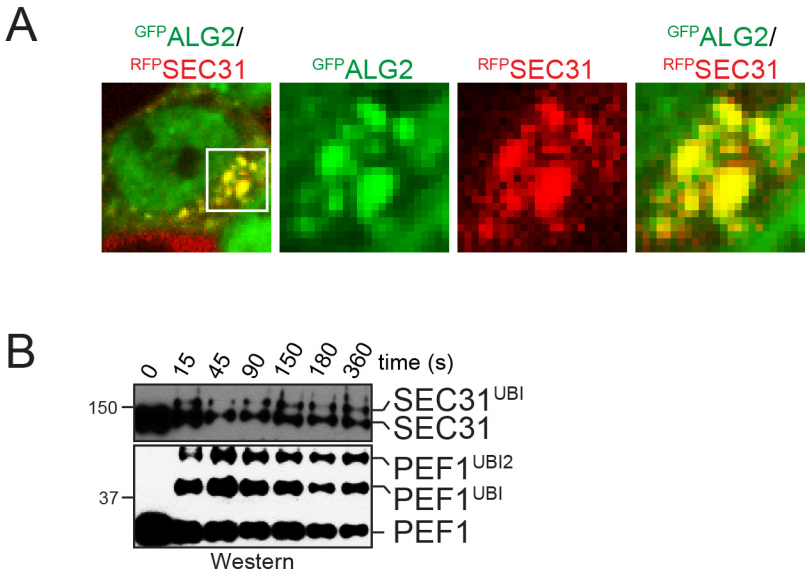

FIGURE S6

Figure S6: CUL3^{KLHL12} is a rapid calcium-dependent ubiquitin ligase. A. Calcium influx caused co-localization of ^{GFP}ALG2 and ^{RFP}SEC31. Shown is a cells at 18s after calcium influx was triggered. **B.** CUL3^{KLHL12} ubiquitylates SEC31 and PEF1 very quickly. Purified PEF1 and SEC31 were incubated with recombinant CUL3^{KLHL12}, ALG2, E1, UBE2D3, ubiquitin, and ATP and incubated at 30C for the indicated times. Ubiquitylation of SEC31 and PEF1 was analyzed by Western blotting.

Chapter 3
Conclusions and Outlook

Conclusions

In this work we have elucidated a novel mechanism by which a CUL3 ubiquitin ligase, $CUL3^{KLHL12}$, is regulated. CUL3 itself functions in a broad spectrum of cellular processes and likely ubiquitylates over a hundred proteins through its association with ~90 distinct substrate receptors (Genschik et al., 2013; Petroski and Deshaies, 2005). CUL3 acts at multiple stages of human development, and activation of complexes between CUL3 and specific substrate adaptors must be tightly controlled. $CUL3^{KLHL12}$, the complex driving collagen secretion, illustrates the need for precise spatial regulation of CUL3 activation. When cells produce and package collagen into COPII vesicles that bud from the ER, $CUL3^{KLHL12}$ must modify SEC31 at ER exit sites, but not in the cytoplasm. Furthermore, the process of collagen packaging inside the ER must be coupled to ubiquitylation at these sites, a process that requires communication across the ER membrane. These requirements illustrate multiple reasons why $CUL3^{KLHL12}$ activity must not be constitutive and must be sensitive to specific aspects of the cellular environment.

We report that collagen trafficking driven by $CUL3^{KLHL12}$ –dependent ubiquitylation of SEC31A requires the target-specific co-adaptor proteins PEF1 and ALG2. Depletion of either of these proteins results in deficient SEC31/$CUL3^{KLHL12}$ binding, SEC31 ubiquitylation, large COPII vesicle formation, and collagen trafficking. PEF1 and ALG2 form a complex and contact the substrate-binding Kelch repeats of KLHL12 via the N-terminal proline/glycine-rich repeats of PEF1. ALG2 then forms a bridge between SEC31 and $CUL3^{KLHL12}$ by directly binding to SEC31. Based on this and previous work, it is likely that SEC31 is targeted by a multimeric $CUL3^{KLHL12}$ ubiquitin ligase in which the substrate is directly engaged by one KLHL12 Kelch propeller and indirectly engaged with an additional Kelch propeller through its interaction with PEF1/ALG2.

PEF1 and ALG2 each contain 5 EF-hand domains, at least 2 of which are known to bind calcium ions (Maki et al., 2011). Calcium binding by the target-specific co-adaptor ALG2 serves as a major point of $CUL3^{KLHL12}$ regulation, as the direct interaction between SEC31 and ALG2 occurs only when ALG2 binds calcium at EF-hand 1 (la Cour et al., 2013; Yamasaki et al., 2006). Accordingly, $CUL3^{KLHL12}$ is unable to target SEC31 when ALG2 is mutated so that it cannot bind calcium, $CUL3^{KLHL12}$-PEF1-ALG2-SEC31 complexes efficiently form only at calcium concentrations >130nM, which is higher than the resting cytosolic calcium concentration and within the physiological range that occurs during waves of ER calcium release.

Calcium-dependent activation of $CUL3^{KLHL12}$ occurs rapidly, suggesting that cellular calcium signaling regulates this ubiquitin ligase. When ER calcium release is induced by ionomycin or histamine treatment, ALG2 relocalizes to SEC31-containing COPII vesicles within ~5 seconds. Upon ionomycin treatment, cytosolic calcium reaches a concentration of 130nM (the concentration at which full $CUL3^{KLHL12}$-PEF1-ALG2-SEC31 complexes assemble *in vitro)* in 5.2 seconds. The agreement between these measurements suggests that $CUL3^{KLHL12}$ is able to target SEC31-containing COPII vesicles within seconds of ER calcium release. This provides a mechanism by which collagen secretion and COPII vesicle trafficking are controlled by signaling pathways that result in increased cytosolic calcium.

The target-specific co-adaptors PEF1 and ALG2 are essential for efficient collagen secretion in cell culture experiments and in organisms. Depletion of PEF1 or ALG2 results in a

profound delay in ER-to-Golgi trafficking of pro-collagen I in human osteosarcoma cells. Similarly, depletion of PEF1 or ALG2 in pro-collagen I-expressing fibrosarcoma cells results in intracellular retention of pro-collagen I. When PEF1 is targeted by morpholino injection, Zebrafish embryos are deficient in craniofacial cartilage, suggesting that there is a collagen secretion defect in craniofacial chondrocytes (data not shown). Based on this data we conclude that calcium-dependent ubiquitylation of SEC31 by $CUL3^{KLHL12}$ is required for proper collagen secretion in organismal development.

Future Directions

Oligomerization and substrate binding by Kelch-like CUL3 substrate receptors

Kelch-like BTB-domain-containing CUL3 substrate receptors are known to recruit substrates to CUL3 via the Kelch domain, which forms a beta propeller structure that binds substrates through loops in between propeller blades. Kelch-like substrate receptors dimerize and bind CUL3 via their BTB domain, likely forming higher-order oligomers when they contain an intervening BACK domain (Errington et al., 2012; Zhuang et al., 2009a). This creates a situation in which a single CUL3 ubiquitin ligase complex contains multiple substrate-binding domains aligned in close proximity to each other. Previous studies have suggested that a single substrate can engage two of these domains at the same time. Multiple KEAP1-binding motifs on the $CUL3^{KEAP1}$ substrate NRF2 allow one NRF2 molecule to contact two KEAP1 polypeptides (McMahon et al., 2006; Tong et al., 2006). Similarly, the CUL3 substrate receptor SPOP binds its substrate, Puc, in a 2:1 ratio (Zhuang et al., 2009a). Our work suggests a related but distinct function of CUL3 substrate receptor dimerization. Here, one KLHL12 Kelch propeller could bind a PEF1-ALG2 co-adaptor complex, and the substrate SEC31 could simultaneously engage the PEF1-ALG2 co-adaptor and the additional free KLHL12 Kelch propeller.

The simplest iteration of this model suggests a KLHL12:PEF1:ALG2:SEC31 ratio of 2:1:1:1, but evidence suggests that active $CUL3^{KLHL12}$ complexes may be significantly larger. Many of these proteins are known to self-associate. KLHL12 can likely form higher-order oligomers through its BACK domain (Errington et al., 2012), ALG2 can likely homo-dimerize (Maki et al., 2011), and SEC31 self-associates extensively as a repeating structural unit of COPII vesicle coats (Stagg et al., 2006). Because of this, biophysical and structural studies will be required to further elucidate the interaction of active $CUL3^{KLHL12}$ with its substrate. In particular, gel filtration and analytical ultracentrifugation could be used to determine the size or sizes of $CUL3^{KLHL12}$ complexes, and electron microscopy could be used to more precisely determine the architecture and molecular arrangement of these complexes.

Models of KLHL12 and KEAP1 suggest functional roles for homo-dimerization of these proteins, but emerging literature also shows potential roles for hetero-dimerization of Kelch-like CUL3 substrate receptors. The highly homologous substrate receptors KLHL9 and KLHL13 function as a heterodimer with roles in mitosis (Sumara et al., 2007). KBTBD6 and KBTBD7 heterodimerize and regulate actin signaling by modulating RAC1 dynamics (Genau et al., 2015). In these cases, KLHL9/13 and KBTBD6/7 pairs share upwards of 90% sequence identity and seem to dimerize with near stoichiometric ratios. Our mass spectrometry detected interactions between KLHL12 and several other CUL3 substrate adaptors including KLHL26, IPP, KLHL2, and KLHL21, suggesting a possible function for KLHL12 hetero-dimerization. However, unlike KLHL9/13 and KBTBD6/7, KLHL12 is significantly divergent from its interacting substrate receptors, and these receptors bind in comparatively low amounts. For these reasons, it is likely

that KLHL12 functions primarily as a homo-oligomer, but the possibility of functional hetero-dimers/oligomers cannot be excluded. Depletion of PEF1 or ALG2 has a significantly stronger effect on collagen trafficking than depletion of KLHL12. This suggests that additional ubiquitin ligases could drive collagen trafficking in the absence of KLHL12. To explore this possibility, it would be useful to examine the interactions of PEF1 and SEC31 by mass spectrometry in the absence of KLHL12 to uncover new interactions with other ubiquitin ligases.

Negative regulation of $CUL3^{KLHL12}$

Experiments using recombinant proteins have demonstrated that $CUL3^{KLHL12}$ can ubiquitylate SEC31 in the absence of PEF1 and ALG2, but these proteins are required for efficient SEC31 ubiquitylation in cellular assays. The discrepancy between these two may lie in the fact that recombinant assays measure ubiquitylation of SEC31 in the absence of other $CUL3^{KLHL12}$ substrates and potential negative regulators. In the crowded cellular environment, $CUL3^{KLHL12}$ could be engaged with other substrates, and SEC31 may be ubiquitylated only when the ligase is maximally activated in the presence of calcium. Similarly, SEC31 is known to be phosphorylated in cells (Koreishi et al., 2013), but the recombinant protein used for our assays is unmodified. SEC31 phosphorylation may be an inhibitory modification, and the additional activity imparted by calcium-dependent activation of $CUL3^{KLHL12}$ may overcome this inhibition. Similarly, this process may be counteracted by deubiquitylating enzymes. In this case, enhanced $CUL3^{KLHL12}$ activity could be required to overcome deubiquitylation activity and promote sustained ubiquitylation of SEC31. Investigating additional regulatory mechanisms such as these will be important to fully understand the mechanism of large COPII vesicle formation by $CUL3^{KLHL12}$.

Biochemical function of ubiquitylation in COPII vesicle trafficking

Once SEC31 is ubiquitylated, this modification must be translated into an increase in vesicle size. The mechanism by which this occurs is currently unknown. The function of SEC31 ubiquitylation could be elucidated in part by determining which region of the protein is modified. Mutational analyses were performed by mutating all lysines of SEC31 to arginine but no single lysine was required for SEC31 ubiquitylation (Jin et al., 2012). However, a cluster of lysines or a particular domain of the protein could be specifically targeted by $CUL3^{KLHL12}$. Further mutational analysis and mass spectrometry could be used the address the question.

SEC31 targeting by $CUL3^{KLHL12}$ could have a variety of consequences depending on the domain that is modified. The N-terminal WD-40 repeats of SEC31 form the junctions of the COPII coat and have some structural flexibility (Zanetti et al., 2013); thus ubiquitylation of this region could directly alter the conformation of the coat and promote a larger lattice of the outer COPII coat. The C-terminal proline-rich domain of SEC31 contacts SEC23, stimulating its GAP activity towards SAR1 and terminating the vesicle budding cycle (Antonny et al., 2001). Ubiquitylation of this region could modulate this interaction and alter the temporal dynamics of COPII vesicle budding, allowing COPII vesicles more time to grow and accommodate pro-collage. Finally, ubiquitylation of any domain of SEC31 could lead to the recruitment of effector proteins that affect COPII biogenesis through a variety of mechanisms.

Determining which region of SEC31 is ubiquitylated would allow for the construction of a constitutively ubiquitylated SEC31 variant with ubiquitin internally fused near its endogenous location or a variant that cannot be ubiquitylated at all. These mutants could be used to test the previously proposed hypotheses with recombinant proteins and in cellular assays.

Broadening the spectrum of calcium-dependent post-translational modifications

Monoubiquitylation is a post-translational modification that has many parallels to phosphorylation. Similar to phosphorylation, attachment of a single ubiquitin can significantly alter a target's interactions with other proteins or intracellular localization (Hicke, 2001). Specifically, calcium-dependent regulation of $CUL3^{KLHL12}$ ubiquitylation activity parallels the calcium-dependent phosphorylation activity of calcium/calmodulin-dependent protein kinases (CAMKs) (Erickson, 2014; Hook and Means, 2001; Lucchesi et al., 2011). This work represents the first example of a calcium-dependent ubiquitin ligase and broadens the parallels between kinase signaling and ubiquitin signaling.

CAMKII is a calcium-dependent kinase involved in neuronal long-term potentiation, learning, memory, and cardiomyocyte function (Erickson, 2014; Lisman et al., 2012; Lucchesi et al., 2011). CAMKII forms a dodecameric ring structure that is autoinhibited at low intracellular calcium concentrations (Rosenberg et al., 2005). When calcium becomes elevated, either through neuronal depolarization or other mechanisms, the EF-hand-containing protein calmodulin binds calcium, which allows it to bind CAMKII. Calmodulin binding relieves autohibition of CAMKs, allowing activation through autophosphorylation and ultimately phosphorylation of target substrates (Lai et al., 1986). Analogous to calmodulin, $CUL3^{KLHL12}$ senses calcium and becomes activated through EF-hand 1 of its co-adaptor protein ALG2. In our model, ALG2 binds SEC31 in response to elevated calcium, facilitating its monoubiquitylation by $CUL3^{KLHL12}$. Dephosphorylation can also be regulated by changes in cellular calcium concentrations. There are at least four major calcium-calmodulin-dependent protein kinases, some with multiple isoforms, that are all activated by calcium-bound calmodulin (Hook and Means, 2001). Conversely, Calcineurin is a calmodulin-dependent serine-threonine protein phosphatase that removes phosphates from target proteins in response to elevated cellular calcium (Rusnak and Mertz, 2000). It is possible that calcium similarly regulates other ubiquitin ligases and deubiquitylating enzymes.

Developmental functions of $CUL3^{KLHL12}$

While the cellular contexts in which CAMKII and other CAMKs become activated are characterized, the calcium-elevating stimulus or stimuli that activate $CUL3^{KLHL12}$ are currently unknown. Based on our data, ER calcium release is sufficient to cause ALG2 relocalization to ER exit sites, but it is not clear whether calcium released from other organelles or imported from the extracellular space can also trigger formation of large collagen-containing COPII vesicles. Furthermore, the specific ion channels that mediate this process and the context in which they become activated are unknown. This may be most easily addressed by first determining the developmental cell types that rely most heavily on $CUL3^{KLHL12}$ activity, and then interrogating the types of calcium signaling events that occur in those cells.

$CUL3^{KLHL12}$ likely has multiple functions in organismal development. It is required to maintain proper morphology of mouse embryonic stem cells through secretion of collagen into the extracellular matrix and is downregulated upon differentiation (Jin et al., 2012). Additionally, its cofactors PEF1 and ALG2 are required for secretion of collagen in a variety of cell types: Depletion of these proteins in osteosarcoma and fibrosarcoma cells suggests they are required for collagen secretion in osteoblasts and fibroblasts. $CUL3^{KLHL12}$ likely contributes to collagen secretion in craniofacial chondrocytes because zebrafish embryos depleted of PEF1 show defects in deposition of craniofacial cartilage. The range of cell types in which KLHL12 and its co-

adaptors PEF1 and ALG2 are expressed is currently unknown, and *in situ* hybridization or immunohistochemistry during development would shed light on this question. Understanding where and when $CUL3^{KLHL12}$ functions will be an important step in understanding the critical process of collagen secretion in organismal development.

References

Alford, A.I., Kozloff, K.M., and Hankenson, K.D. (2015). Extracellular matrix networks in bone remodeling. Int J Biochem Cell Biol *65*, 20-31.

Angers, S., Thorpe, C.J., Biechele, T.L., Goldenberg, S.J., Zheng, N., MacCoss, M.J., and Moon, R.T. (2006). The KLHL12-Cullin-3 ubiquitin ligase negatively regulates the Wnt-beta-catenin pathway by targeting Dishevelled for degradation. Nature cell biology *8*, 348-357.

Antonny, B., Madden, D., Hamamoto, S., Orci, L., and Schekman, R. (2001). Dynamics of the COPII coat with GTP and stable analogues. Nature cell biology *3*, 531-537.

Betancur, P., Bronner-Fraser, M., and Sauka-Spengler, T. (2010). Assembling neural crest regulatory circuits into a gene regulatory network. Annu Rev Cell Dev Biol *26*, 581-603.

Boyadjiev, S.A., Fromme, J.C., Ben, J., Chong, S.S., Nauta, C., Hur, D.J., Zhang, G., Hamamoto, S., Schekman, R., Ravazzola, M.*, et al.* (2006). Cranio-lenticulo-sutural dysplasia is caused by a SEC23A mutation leading to abnormal endoplasmic-reticulum-to-Golgi trafficking. Nat Genet *38*, 1192-1197.

Chen, S., Desai, T., McNew, J.A., Gerard, P., Novick, P.J., and Ferro-Novick, S. (2015). Lunapark stabilizes nascent three-way junctions in the endoplasmic reticulum. Proc Natl Acad Sci U S A *112*, 418-423.

Cinque, L., Forrester, A., Bartolomeo, R., Svelto, M., Venditti, R., Montefusco, S., Polishchuk, E., Nusco, E., Rossi, A., Medina, D.L.*, et al.* (2015). FGF signalling regulates bone growth through autophagy. Nature.

Clapham, D.E. (2007). Calcium signaling. Cell *131*, 1047-1058.

Dauwerse, J.G., Dixon, J., Seland, S., Ruivenkamp, C.A., van Haeringen, A., Hoefsloot, L.H., Peters, D.J., Boers, A.C., Daumer-Haas, C., Maiwald, R.*, et al.* (2011). Mutations in genes encoding subunits of RNA polymerases I and III cause Treacher Collins syndrome. Nat Genet *43*, 20-22.

De Rubeis, S., He, X., Goldberg, A.P., Poultney, C.S., Samocha, K., Cicek, A.E., Kou, Y., Liu, L., Fromer, M., Walker, S.*, et al.* (2014). Synaptic, transcriptional and chromatin genes disrupted in autism. Nature *515*, 209-215.

Dixon, J., and Dixon, M.J. (2004). Genetic background has a major effect on the penetrance and severity of craniofacial defects in mice heterozygous for the gene encoding the nucleolar protein Treacle. Developmental dynamics : an official publication of the American Association of Anatomists *229*, 907-914.

Dou, H., Buetow, L., Sibbet, G.J., Cameron, K., and Huang, D.T. (2012). BIRC7-E2 ubiquitin conjugate structure reveals the mechanism of ubiquitin transfer by a RING dimer. Nature structural & molecular biology *19*, 876-883.

Duda, D.M., Scott, D.C., Calabrese, M.F., Zimmerman, E.S., Zheng, N., and Schulman, B.A. (2011). Structural regulation of cullin-RING ubiquitin ligase complexes. Curr Opin Struct Biol *21*, 257-264.

Eletr, Z.M., Huang, D.T., Duda, D.M., Schulman, B.A., and Kuhlman, B. (2005). E2 conjugating enzymes must disengage from their E1 enzymes before E3-dependent ubiquitin and ubiquitin-like transfer. Nature structural & molecular biology *12*, 933-934.

Erickson, J.R. (2014). Mechanisms of CaMKII Activation in the Heart. Frontiers in pharmacology *5*, 59.

Errington, W.J., Khan, M.Q., Bueler, S.A., Rubinstein, J.L., Chakrabartty, A., and Prive, G.G. (2012). Adaptor protein self-assembly drives the control of a cullin-RING ubiquitin ligase. Structure (London, England : 1993) *20*, 1141-1153.

Ewald, C.Y., Landis, J.N., Porter Abate, J., Murphy, C.T., and Blackwell, T.K. (2015). Dauer-independent insulin/IGF-1-signalling implicates collagen remodelling in longevity. Nature *519*, 97-101.

Fath, S., Mancias, J.D., Bi, X., and Goldberg, J. (2007). Structure and organization of coat proteins in the COPII cage. Cell *129*, 1325-1336.

Fromme, J.C., Ravazzola, M., Hamamoto, S., Al-Balwi, M., Eyaid, W., Boyadjiev, S.A., Cosson, P., Schekman, R., and Orci, L. (2007). The genetic basis of a craniofacial disease provides insight into COPII coat assembly. Dev Cell *13*, 623-634.

Furukawa, M., He, Y.J., Borchers, C., and Xiong, Y. (2003). Targeting of protein ubiquitination by BTB-Cullin 3-Roc1 ubiquitin ligases. Nat Cell Biol *5*, 1001-1007.

Genau, H.M., Huber, J., Baschieri, F., Akutsu, M., Dotsch, V., Farhan, H., Rogov, V., and Behrends, C. (2015). CUL3-KBTBD6/KBTBD7 ubiquitin ligase cooperates with GABARAP proteins to spatially restrict TIAM1-RAC1 signaling. Molecular cell *57*, 995-1010.

Genschik, P., Sumara, I., and Lechner, E. (2013). The emerging family of CULLIN3-RING ubiquitin ligases (CRL3s): cellular functions and disease implications. The EMBO journal *32*, 2307-2320.

Geyer, R., Wee, S., Anderson, S., Yates, J., and Wolf, D.A. (2003). BTB/POZ domain proteins are putative substrate adaptors for cullin 3 ubiquitin ligases. Mol Cell *12*, 783-790.

Gillon, A.D., Latham, C.F., and Miller, E.A. (2012). Vesicle-mediated ER export of proteins and lipids. Biochim Biophys Acta *1821*, 1040-1049.

Green, S.A., Simoes-Costa, M., and Bronner, M.E. (2015). Evolution of vertebrates as viewed from the crest. Nature *520*, 474-482.

Gschweitl, M., Ulbricht, A., Barnes, C.A., Enchev, R.I., Stoffel-Studer, I., Meyer-Schaller, N., Huotari, J., Yamauchi, Y., Greber, U.F., Helenius, A.*, et al.* (2016). A SPOPL/Cullin-3 ubiquitin ligase complex regulates endocytic trafficking by targeting EPS15 at endosomes. Elife *5*.

Hicke, L. (2001). Protein regulation by monoubiquitin. Nature reviews Molecular cell biology *2*, 195-201.

Hook, S.S., and Means, A.R. (2001). Ca(2+)/CaM-dependent kinases: from activation to function. Annual review of pharmacology and toxicology *41*, 471-505.

Huttlin, E.L., Ting, L., Bruckner, R.J., Gebreab, F., Gygi, M.P., Szpyt, J., Tam, S., Zarraga, G., Colby, G., Baltier, K.*, et al.* (2015). The BioPlex Network: A Systematic Exploration of the Human Interactome. Cell *162*, 425-440.

Jensen, D., and Schekman, R. (2011). COPII-mediated vesicle formation at a glance. Journal of cell science *124*, 1-4.

Jia, J., Tarabykina, S., Hansen, C., Berchtold, M., and Cygler, M. (2001). Structure of apoptosis-linked protein ALG-2: insights into Ca2+-induced changes in penta-EF-hand proteins. Structure *9*, 267-275.

Jin, L., Pahuja, K.B., Wickliffe, K.E., Gorur, A., Baumgartel, C., Schekman, R., and Rape, M. (2012). Ubiquitin-dependent regulation of COPII coat size and function. Nature *482*, 495-500.
Karsenty, G., Kronenberg, H.M., and Settembre, C. (2009). Genetic control of bone formation. Annu Rev Cell Dev Biol *25*, 629-648.

Koreishi, M., Yu, S., Oda, M., Honjo, Y., and Satoh, A. (2013). CK2 phosphorylates Sec31 and regulates ER-To-Golgi trafficking. PLoS One *8*, e54382.

Kovacs, J.J., Hara, M.R., Davenport, C.L., Kim, J., and Lefkowitz, R.J. (2009). Arrestin development: emerging roles for beta-arrestins in developmental signaling pathways. Dev Cell *17*, 443-458.

la Cour, J.M., Mollerup, J., and Berchtold, M.W. (2007). ALG-2 oscillates in subcellular localization, unitemporally with calcium oscillations. Biochem Biophys Res Commun *353*, 1063-1067.

la Cour, J.M., Schindler, A.J., Berchtold, M.W., and Schekman, R. (2013). ALG-2 attenuates COPII budding in vitro and stabilizes the Sec23/Sec31A complex. PLoS One *8*, e75309.

Lai, Y., Nairn, A.C., and Greengard, P. (1986). Autophosphorylation reversibly regulates the Ca2+/calmodulin-dependence of Ca2+/calmodulin-dependent protein kinase II. Proceedings of the National Academy of Sciences of the United States of America *83*, 4253-4257.

Lang, M.R., Lapierre, L.A., Frotscher, M., Goldenring, J.R., and Knapik, E.W. (2006). Secretory COPII coat component Sec23a is essential for craniofacial chondrocyte maturation. Nat Genet *38*, 1198-1203.

Langeberg, L.K., and Scott, J.D. (2015). Signalling scaffolds and local organization of cellular behaviour. Nat Rev Mol Cell Biol *16*, 232-244.

Lee, T.I., and Young, R.A. (2013). Transcriptional regulation and its misregulation in disease. Cell *152*, 1237-1251.

Lin, S.S., Tzeng, B.H., Lee, K.R., Smith, R.J., Campbell, K.P., and Chen, C.C. (2014). Cav3.2 T-type calcium channel is required for the NFAT-dependent Sox9 expression in tracheal cartilage. Proc Natl Acad Sci U S A *111*, E1990-1998.

Lisman, J., Yasuda, R., and Raghavachari, S. (2012). Mechanisms of CaMKII action in long-term potentiation. Nature reviews Neuroscience *13*, 169-182.

Liu, C.C., Lin, Y.C., Chen, Y.H., Chen, C.M., Pang, L.Y., Chen, H.A., Wu, P.R., Lin, M.Y., Jiang, S.T., Tsai, T.F.*, et al.* (2016). Cul3-KLHL20 Ubiquitin Ligase Governs the Turnover of ULK1 and VPS34 Complexes to Control Autophagy Termination. Molecular cell *61*, 84-97.

Louis-Dit-Picard, H., Barc, J., Trujillano, D., Miserey-Lenkei, S., Bouatia-Naji, N., Pylypenko, O., Beaurain, G., Bonnefond, A., Sand, O., Simian, C.*, et al.* (2012). KLHL3 mutations cause familial hyperkalemic hypertension by impairing ion transport in the distal nephron. Nat Genet *44*, 456-460, S451-453.

Lu, A., and Pfeffer, S.R. (2013). Golgi-associated RhoBTB3 targets cyclin E for ubiquitylation and promotes cell cycle progression. J Cell Biol *203*, 233-250.

Lucchesi, W., Mizuno, K., and Giese, K.P. (2011). Novel insights into CaMKII function and regulation during memory formation. Brain research bulletin *85*, 2-8.

Lydeard, J.R., Schulman, B.A., and Harper, J.W. (2013). Building and remodelling Cullin-RING E3 ubiquitin ligases. EMBO reports *14*, 1050-1061.

Maerki, S., Olma, M.H., Staubli, T., Steigemann, P., Gerlich, D.W., Quadroni, M., Sumara, I., and Peter, M. (2009). The Cul3-KLHL21 E3 ubiquitin ligase targets aurora B to midzone microtubules in anaphase and is required for cytokinesis. The Journal of cell biology *187*, 791-800.

Maki, M., Suzuki, H., and Shibata, H. (2011). Structure and function of ALG-2, a penta-EF-hand calcium-dependent adaptor protein. Science China Life sciences *54*, 770-779.

Malhotra, V., and Erlmann, P. (2015). The Pathway of Collagen Secretion. Annu Rev Cell Dev Biol *31*, 109-124.

Matsuoka, K., Orci, L., Amherdt, M., Bednarek, S.Y., Hamamoto, S., Schekman, R., and Yeung, T. (1998). COPII-coated vesicle formation reconstituted with purified coat proteins and chemically defined liposomes. Cell *93*, 263-275.

McMahon, M., Thomas, N., Itoh, K., Yamamoto, M., and Hayes, J.D. (2006). Dimerization of substrate adaptors can facilitate cullin-mediated ubiquitylation of proteins by a "tethering" mechanism: a two-site interaction model for the Nrf2-Keap1 complex. The Journal of biological chemistry *281*, 24756-24768.

Metzger, M.B., Hristova, V.A., and Weissman, A.M. (2012). HECT and RING finger families of E3 ubiquitin ligases at a glance. Journal of cell science *125*, 531-537.

Miller, E., Antonny, B., Hamamoto, S., and Schekman, R. (2002). Cargo selection into COPII vesicles is driven by the Sec24p subunit. The EMBO journal *21*, 6105-6113.

Miller, E.A., Beilharz, T.H., Malkus, P.N., Lee, M.C., Hamamoto, S., Orci, L., and Schekman, R. (2003). Multiple cargo binding sites on the COPII subunit Sec24p ensure capture of diverse membrane proteins into transport vesicles. Cell *114*, 497-509.

Petersen, O.H. (2015). Ca(2)(+) signalling in the endoplasmic reticulum/secretory granule microdomain. Cell Calcium *58*, 397-404.

Petroski, M.D., and Deshaies, R.J. (2005). Function and regulation of cullin-RING ubiquitin ligases. Nature reviews Molecular cell biology *6*, 9-20.

Pintard, L., Willis, J.H., Willems, A., Johnson, J.L., Srayko, M., Kurz, T., Glaser, S., Mains, P.E., Tyers, M., Bowerman, B.*, et al.* (2003). The BTB protein MEL-26 is a substrate-specific adaptor of the CUL-3 ubiquitin-ligase. Nature *425*, 311-316.

Plechanovova, A., Jaffray, E.G., Tatham, M.H., Naismith, J.H., and Hay, R.T. (2012). Structure of a RING E3 ligase and ubiquitin-loaded E2 primed for catalysis. Nature *489*, 115-120.

Pruneda, J.N., Littlefield, P.J., Soss, S.E., Nordquist, K.A., Chazin, W.J., Brzovic, P.S., and Klevit, R.E. (2012). Structure of an E3:E2~Ub complex reveals an allosteric mechanism shared among RING/U-box ligases. Molecular cell *47*, 933-942.

Rahighi, S., and Dikic, I. (2012). Selectivity of the ubiquitin-binding modules. FEBS letters *586*, 2705-2710.

Ravenscroft, G., Miyatake, S., Lehtokari, V.L., Todd, E.J., Vornanen, P., Yau, K.S., Hayashi, Y.K., Miyake, N., Tsurusaki, Y., Doi, H.*, et al.* (2013). Mutations in KLHL40 are a frequent cause of severe autosomal-recessive nemaline myopathy. American journal of human genetics *93*, 6-18.

Rhinn, H., Fujita, R., Qiang, L., Cheng, R., Lee, J.H., and Abeliovich, A. (2013). Integrative genomics identifies APOE epsilon4 effectors in Alzheimer's disease. Nature *500*, 45-50.

Rizzuto, R., and Pozzan, T. (2006). Microdomains of intracellular Ca2+: molecular determinants and functional consequences. Physiol Rev *86*, 369-408.

Rosenberg, O.S., Deindl, S., Sung, R.J., Nairn, A.C., and Kuriyan, J. (2005). Structure of the autoinhibited kinase domain of CaMKII and SAXS analysis of the holoenzyme. Cell *123*, 849-860.

Rusnak, F., and Mertz, P. (2000). Calcineurin: form and function. Physiological reviews *80*, 1483-1521.

Saito, K., Chen, M., Bard, F., Chen, S., Zhou, H., Woodley, D., Polischuk, R., Schekman, R., and Malhotra, V. (2009). TANGO1 facilitates cargo loading at endoplasmic reticulum exit sites. Cell *136*, 891-902.

Saito, K., Yamashiro, K., Ichikawa, Y., Erlmann, P., Kontani, K., Malhotra, V., and Katada, T. (2011). cTAGE5 mediates collagen secretion through interaction with TANGO1 at endoplasmic reticulum exit sites. Molecular biology of the cell *22*, 2301-2308.

Schulman, B.A., and Harper, J.W. (2009). Ubiquitin-like protein activation by E1 enzymes: the apex for downstream signalling pathways. Nat Rev Mol Cell Biol *10*, 319-331.

Schwanhausser, B., Busse, D., Li, N., Dittmar, G., Schuchhardt, J., Wolf, J., Chen, W., and Selbach, M. (2011). Global quantification of mammalian gene expression control. Nature *473*, 337-342.

Scott, D.C., Monda, J.K., Bennett, E.J., Harper, J.W., and Schulman, B.A. (2011). N-terminal acetylation acts as an avidity enhancer within an interconnected multiprotein complex. Science *334*, 674-678.

Sheard, L.B., Tan, X., Mao, H., Withers, J., Ben-Nissan, G., Hinds, T.R., Kobayashi, Y., Hsu, F.F., Sharon, M., Browse, J.*, et al.* (2010). Jasmonate perception by inositol-phosphate-potentiated COI1-JAZ co-receptor. Nature *468*, 400-405.

Smith, S.M., Garic, A., Berres, M.E., and Flentke, G.R. (2014). Genomic factors that shape craniofacial outcome and neural crest vulnerability in FASD. Front Genet *5*, 224.

Soret, R., Mennetrey, M., Bergeron, K.F., Dariel, A., Neunlist, M., Grunder, F., Faure, C., Silversides, D.W., and Pilon, N. (2015). A collagen VI-dependent pathogenic mechanism for Hirschsprung's disease. The Journal of clinical investigation.

Sowa, M.E., Bennett, E.J., Gygi, S.P., and Harper, J.W. (2009). Defining the human deubiquitinating enzyme interaction landscape. Cell *138*, 389-403.

Stagg, S.M., Gurkan, C., Fowler, D.M., LaPointe, P., Foss, T.R., Potter, C.S., Carragher, B., and Balch, W.E. (2006). Structure of the Sec13/31 COPII coat cage. Nature *439*, 234-238.

Stratton, M.M., Chao, L.H., Schulman, H., and Kuriyan, J. (2013). Structural studies on the regulation of Ca2+/calmodulin dependent protein kinase II. Curr Opin Struct Biol *23*, 292-301.

Sumara, I., Quadroni, M., Frei, C., Olma, M.H., Sumara, G., Ricci, R., and Peter, M. (2007). A Cul3-based E3 ligase removes Aurora B from mitotic chromosomes, regulating mitotic progression and completion of cytokinesis in human cells. Developmental cell *12*, 887-900.

Taipale, M., Tucker, G., Peng, J., Krykbaeva, I., Lin, Z.Y., Larsen, B., Choi, H., Berger, B., Gingras, A.C., and Lindquist, S. (2014). A quantitative chaperone interaction network reveals the architecture of cellular protein homeostasis pathways. Cell *158*, 434-448.

Takahashi, T., Kojima, K., Zhang, W., Sasaki, K., Ito, M., Suzuki, H., Kawasaki, M., Wakatsuki, S., Takahara, T., Shibata, H.*, et al.* (2015). Structural analysis of the complex between penta-EF-hand ALG-2 protein and Sec31A peptide reveals a novel target recognition mechanism of ALG-2. Int J Mol Sci *16*, 3677-3699.

Tan, X., Calderon-Villalobos, L.I., Sharon, M., Zheng, C., Robinson, C.V., Estelle, M., and Zheng, N. (2007). Mechanism of auxin perception by the TIR1 ubiquitin ligase. Nature *446*, 640-645.

Tomita, M., Reinhold, M.I., Molkentin, J.D., and Naski, M.C. (2002). Calcineurin and NFAT4 induce chondrogenesis. J Biol Chem *277*, 42214-42218.

Tong, K.I., Katoh, Y., Kusunoki, H., Itoh, K., Tanaka, T., and Yamamoto, M. (2006). Keap1 recruits Neh2 through binding to ETGE and DLG motifs: characterization of the two-site molecular recognition model. Molecular and cellular biology *26*, 2887-2900.

Twigg, S.R., and Wilkie, A.O. (2015). New insights into craniofacial malformations. Hum Mol Genet *24*, R50-59.

Venditti, R., Scanu, T., Santoro, M., Di Tullio, G., Spaar, A., Gaibisso, R., Beznoussenko, G.V., Mironov, A.A., Mironov, A., Jr., Zelante, L.*, et al.* (2012). Sedlin controls the ER export of procollagen by regulating the Sar1 cycle. Science *337*, 1668-1672.

Wang, M., and Kaufman, R.J. (2014). The impact of the endoplasmic reticulum protein-folding environment on cancer development. Nat Rev Cancer *14*, 581-597.

Werner, A., Iwasaki, S., McGourty, C.A., Medina-Ruiz, S., Teerikorpi, N., Fedrigo, I., Ingolia, N.T., and Rape, M. (2015). Cell-fate determination by ubiquitin-dependent regulation of translation. Nature *525*, 523-527.

White, R.M., Cech, J., Ratanasirintrawoot, S., Lin, C.Y., Rahl, P.B., Burke, C.J., Langdon, E., Tomlinson, M.L., Mosher, J., Kaufman, C.*, et al.* (2011). DHODH modulates transcriptional elongation in the neural crest and melanoma. Nature *471*, 518-522.

Wickliffe, K.E., Lorenz, S., Wemmer, D.E., Kuriyan, J., and Rape, M. (2011). The mechanism of linkage-specific ubiquitin chain elongation by a single-subunit e2. Cell *144*, 769-781.

Wilson, S.R., Gerhold, K.A., Bifolck-Fisher, A., Liu, Q., Patel, K.N., Dong, X., and Bautista, D.M. (2011). TRPA1 is required for histamine-independent, Mas-related G protein-coupled receptor-mediated itch. Nat Neurosci *14*, 595-602.

Xu, L., Wei, Y., Reboul, J., Vaglio, P., Shin, T.H., Vidal, M., Elledge, S.J., and Harper, J.W. (2003). BTB proteins are substrate-specific adaptors in an SCF-like modular ubiquitin ligase containing CUL-3. Nature *425*, 316-321.

Yamasaki, A., Tani, K., Yamamoto, A., Kitamura, N., and Komada, M. (2006). The Ca2+-binding protein ALG-2 is recruited to endoplasmic reticulum exit sites by Sec31A and stabilizes the localization of Sec31A. Molecular biology of the cell *17*, 4876-4887.

Yoshibori, M., Yorimitsu, T., and Sato, K. (2012). Involvement of the penta-EF-hand protein Pef1p in the Ca2+-dependent regulation of COPII subunit assembly in Saccharomyces cerevisiae. PLoS One *7*, e40765.

Yuan, W.C., Lee, Y.R., Lin, S.Y., Chang, L.Y., Tan, Y.P., Hung, C.C., Kuo, J.C., Liu, C.H., Lin, M.Y., Xu, M.*, et al.* (2014). K33-Linked Polyubiquitination of Coronin 7 by Cul3-KLHL20 Ubiquitin E3 Ligase Regulates Protein Trafficking. Molecular cell *54*, 586-600.

Zanetti, G., Prinz, S., Daum, S., Meister, A., Schekman, R., Bacia, K., and Briggs, J.A. (2013). The structure of the COPII transport-vesicle coat assembled on membranes. eLife *2*, e00951.

Zhang, T., Dong, K., Liang, W., Xu, D., Xia, H., Geng, J., Najafov, A., Liu, M., Li, Y., Han, X.*, et al.* (2015). G-protein-coupled receptors regulate autophagy by ZBTB16-mediated ubiquitination and proteasomal degradation of Atg14L. Elife *4*, e06734.

Zhou, Z., Xu, C., Chen, P., Liu, C., Pang, S., Yao, X., and Zhang, Q. (2015). Stability of HIB-Cul3 E3 ligase adaptor HIB Is Regulated by Self-degradation and Availability of Its Substrates. Sci Rep *5*, 12709.

Zhuang, M., Calabrese, M.F., Liu, J., Waddell, M.B., Nourse, A., Hammel, M., Miller, D.J., Walden, H., Duda, D.M., Seyedin, S.N.*, et al.* (2009a). Structures of SPOP-substrate complexes: insights into molecular architectures of BTB-Cul3 ubiquitin ligases. Molecular cell *36*, 39-50.

Zhuang, M., Calabrese, M.F., Liu, J., Waddell, M.B., Nourse, A., Hammel, M., Miller, D.J., Walden, H., Duda, D.M., Seyedin, S.N.*, et al.* (2009b). Structures of SPOP-substrate complexes: insights into molecular architectures of BTB-Cul3 ubiquitin ligases. Molecular cell *36*, 39-50.